Acquisition of Optimum Co-sources of Sulfur MAA Capped-ZnS Quantum Dots Conditions for Photoluminescence Chlorine Sensor

Jehan Elnady
City of Scientific Research and Technological Applications
Tosson Shaala
Institute of Graduate Studies and Research
Moataz Soliman
Institute of Graduate Studies and Research
Shaker Ebrahim
Institute of Graduate Studies and Research
ahmed elshaer (ahshaer@alexu.edu.eg)
Higher Institute of Engineering & Technology-ElBohira https://orcid.org/0000-0001-8457-1051

Research Article

Keywords: ZnS, Quantum dots, Chlorine, Sensor, Mercaptoacetic acid

Posted Date: March 24th, 2021

DOI: https://doi.org/10.21203/rs.3.rs-337950/v1

Acquisition of optimum co-sources of sulfur MAA capped-ZnS quantum dots conditions for photoluminescence chlorine sensor

Jehan Elnady[1], Tosson Shaala[2], Moataz Soliman[2], Shaker Ebrahim[2], A.M. Elshaer[3]

[1]Electronic Materials Department, Advanced Technology and New Materials Research Institute, City of Scientific Research and Technological Applications (SRTA-City), New Borg El-Arab City, P.O. Box 21934, Alexandria, Egypt.

[2]Department of Materials Science, Institute of Graduate Studies and Research, Alexandria University, 163 Horrya Avenue, El-Shatby, P.O.Box 832, Alexandria, Egypt.
[3]Higher Institute of Engineering and Technology, El-Boheira, Egypt. P.O.Box 22751, El-Boheira, Egypt. ahshaer@alexu.edu.eg

Abstract

ZnS quantum dots (QDs) has received a great attention due to its unique properties and wide applications. The objective of this work is to synthesize ZnS QDs by hydrothermal method and capped with mercaptoacetic acid (MAA) to be used as a chlorine sensor in the range from 1 to 35 mg/L. Optical, structural and morphological properties of MAA capped-ZnS QDs were investigated. MAA capped-ZnS QDs exhibited a cubic structure with an average diameter size of 8.8 nm. Photoluminescence (PL) spectra of the fabricated MAA capped-ZnS QDs revealed three basic emission peaks at 371, 423 and 486 nm due to level transitions involving of zinc vacancy, interstitial sulfur and zinc, respectively. The photostability of the MAA capped-ZnS QDs was examined after 14 months which retains 12% of the original PL intensity without any peak shift. The MAA capped-ZnS QDs PL intensity was changed linearly with the chlorine concentration in the range from 1 to 35 mg/L with correlation coefficient, sensitivity and limit of detection of 0.9782, 6.96×10^{-2} ppm^{-1} and 3.6 mg/L, respectively.

Keywords: ZnS; Quantum dots; Chlorine; Sensor; Mercaptoacetic acid

1. Introduction

The charge and energy of small particles of some semiconductor materials are quantized just like those of an atom and the quantum dot reveals atom-like features. QDs nanocrystals have unique chemical and physical properties that differ from those of the bulk. QDs exhibit interested electrooptical properties like size tunable-light emission, immense signal-brightness and long-term photostability [1-2]. QDs have many different applications such as sensors [3,4], light-emitting diodes [5] and solar cells [6]. Chlorine,

hypochlorous acid, and hypochlorite are used as disinfectants in water treatment process to remove pathogenic bacteria, viruses, and microorganisms [7,8]. High excess of chlorine ions in water is harmful to human health and must be avoided [9]. Various conventional sensing techniques have been developed to estimate exact chlorine concentration such as electrochemical, optical, and chemiluminescence sensors [10-12]. These techniques are accompanied by some challenges like poor selectivity and low detection limit. Optical sensors based on nanoparticles have been developed for the detection of free chlorine having several advantages compared with the previous techniques [13-16]. ZnS is an outstanding semiconductor with a large bandgap has a cubic-structure and is chemically more stable, nontoxic and environmentally safe than compound semiconductors [17-19]. Hence, it has more potential applications in biological detection and wastewater treatment [20]. ZnS QDs have been fabricated using different techniques such as micro-emulsion [21], hot injection [22], vapor deposition [23], sol–gel [24], hydrothermal [25] and facile one step method [26].

The effect of temperature, pH, Zn^{2+}:S^{2-} molar ratio, reaction time, sulfur source, and MAA:thiourea ratio on the optical, structural and morphological properties of the synthesized hydrothermal MAA capped-ZnS QDs is investigated and studied. The fluorescence sensor based on MAA capped-ZnS QDs for free chlorine in the range of 1 to 35 mg/L is applied. The corresponding output of photoluminescence spectra provides a feasible method to quantify and calibrate the relationship between free chlorine concentrations and emission peak intensity. The proposed mechanism of the interactions between free chlorine and MAA capped-ZnS QDs is suggested.

2. Materials and Methods

2.1. Materials

Zinc acetate dehydrate ($Zn(CH_3COO)_2.2H_2O$,99%), sodium sulphide ($Na_2S.6H_2O$, 30%), and thioglycolic acid (TGA) were purchased from Oxford Laboratory, research-lab chemical industries, Merck Schuchardt OHG, India, respectively. Thiourea and ethanol were brought from Elnasr pharmaceutical chemical CO, Egypt. Ammonia was received from Fisher UK Company, UK. Sodium hypochlorite (NaClO) was purchased from Egyptian petrochemical company, Egypt. All solutions were synthesized with water purified by a Millipore Milli-Q purification system.

2.2. Preparation of MAA capped-ZnS QDs as chlorine sensor

The MAA capped-ZnS QDs were synthesized by the hydrothermal method with MAA as a capping molecule in aqueous media as shown in Figure 1. Firstly, dissolving 1.32 g of $Zn(CH_3COO)_2.2H_2O$ in 50 mL of DI water. Secondly, 4.5 mL of MAA was slowly added to the solution with stirring for 10 min. 2.16 g of $Na_2S.6H_2O$ dissolved in 5 mL of DI water was added to the mixture and the stirring continued until a clear solution was obtained. After 5 mL of 0.9 mol/L thiourea solution was dropped and the pH of the mixture was adjusted to 9 with aqueous ammonia, the liquid was transferred into a 100 mL Teflon-lined stainless-steel autoclave. Hydrothermal treatment was carried out at 125°C for 2 hrs. The autoclave was then left to cool down to room temperature. The QDs solution was added to ethyl alcohol, then precipitated QDs were separated by centrifugation at 6,500 rpm for 6 min and this step was repeated several times to remove unreacted materials.

The prepared MAA capped-ZnS QDs were dispersed in distilled water for the detection of free chlorine. Stock solution of hypochlorite was used as a source of free chlorine. Before the experiment, standardization of hypochlorite solution was done by iodometric titration. Solutions of different concentrations of free chlorine from 1 to 35 ppm and a fixed concentration of MAA capped-ZnS QDs were prepared and measured the fluorescence spectra for detection of the free chlorine concentration.

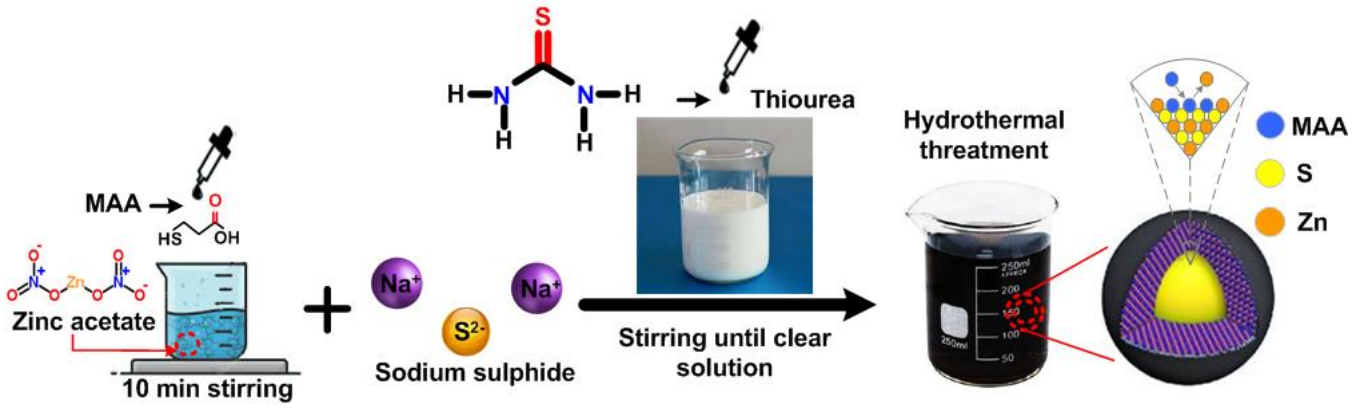

Figure 1. preparation steps diagram of MAA capped-ZnS QDs.

2.3 Characterization techniques

UV-visible absorption of the MAA capped-ZnS QDs solution is carried out using Thermo scientific Evolution 300 UV-vis spectrophotometer in the wavelength range from 260 nm to 600 nm. The size, morphology and homogeneity of the prepared QDs were determined based on JEOL (JEM 2100F) microscope equipped with field emission gun at an accelerating voltage 200 kV was used for HRTEM

analysis of samples. X-ray diffraction was performed using (X-ray 7000 Shimadzu-Japan) at room temperature in the range of 2θ from 10 to 80 degree to determine the degree of crystallinity of MAA capped-ZnS QDs. The X-ray source Cu target generated at 30 kV and 30 mA with scan speed of 4 deg/min. PL emission spectra of MAA capped-ZnS QDs solution were recorded from 290 nm to 600 nm excited at 270 nm using a Perkin Elmer LS-55 Fluorescence Spectrometer. Energy band gap (E_g) was calculated from Tauc's plot $\alpha h\upsilon = K (h\upsilon - E_g)^n$,where $h\upsilon$ is the photon energy in eV, α is absorption coefficient and K is a constant, which depends on the nature of the transition [16,27].

3. Results and Discussion

3.1. Optical absorbance properties of MAA capped-ZnS QDs

The effect of temperature, pH, Zn^{2+}:S^{2-} molar ratio, time, sulfur source, and MAA/thiourea on photoluminescence (PL) emission is investigated to acquire the optimum preparation parameters of MAA capped-ZnS QDs as chlorine sensor. The reaction temperature and pH value control the nucleation rate which are vital factors for the quality of the QDs [28]. Figure 2 shows the effect of temperature is studied at 100, 125, 150, 175, and 200°C in order to obtain the optimum temperature for synthesis of MAA capped-ZnS QDs. Blue shift is observed from 315 to 305 as the temperature increase from 100 to 125°C, respectively due to increasing the monomers concentration which take part in interfacial nucleation resulting in particle size reduction [28,29]. The spectra are red shifted again to 320 nm by increasing the temperature to 150°C due to dissociation of capping agent leading to aggregated of MAA capped-ZnS QDs [30,31]. At temperatures of 175°C and 200°C a precipitation of MAA capped-ZnS QDs is occurred as shown in the inset of Figure 2. It is observed that MAA capped-ZnS QDs prepared at 125°C have a higher luminance peak at 365 nm than MAA capped-ZnS QDs prepared at 100°C and 150°C. The increment of reaction temperature from 100°C to 125°C has a critical effect on the PL spectra of the synthesized MAA capped-ZnS QDs. The moderate increment in temperature from 100°C to 125°C influences the association of the MAA capped-ZnS complex, prompting the enhancement of the free monomer concentration in the subsequent growth [28,32]. When the temperature increases to 150 °C, the rate of the dissociation of the ligands from the MAA capped-ZnS QDs surface is quickened and prompting a growth of the crystals of MAA capped-ZnS QDs without stabilizers [33]. At 150°C, it expected that there are fewer ligands onto the surface sites, and more surface defects are created due to the lower coverage provided by the ligands, proposing that there existed a specific amount of dangling bonds at the

surface of the MAA capped-ZnS QDs [34]. Consequently, at temperatures 175°C and 200°C precipitation of MAA capped-ZnS QDs is occurred. Therefore, the optical properties of the MAA capped-ZnS QDs are declined. The band gap values of the prepared MAA capped-ZnS QDs at different temperature are estimated based on the Tauc's plot which are about 3.85eV, 3.88 eV and 3.83 eV for MAA capped-ZnS QDs prepared at 100°C, 125°C and 150°C respectively.

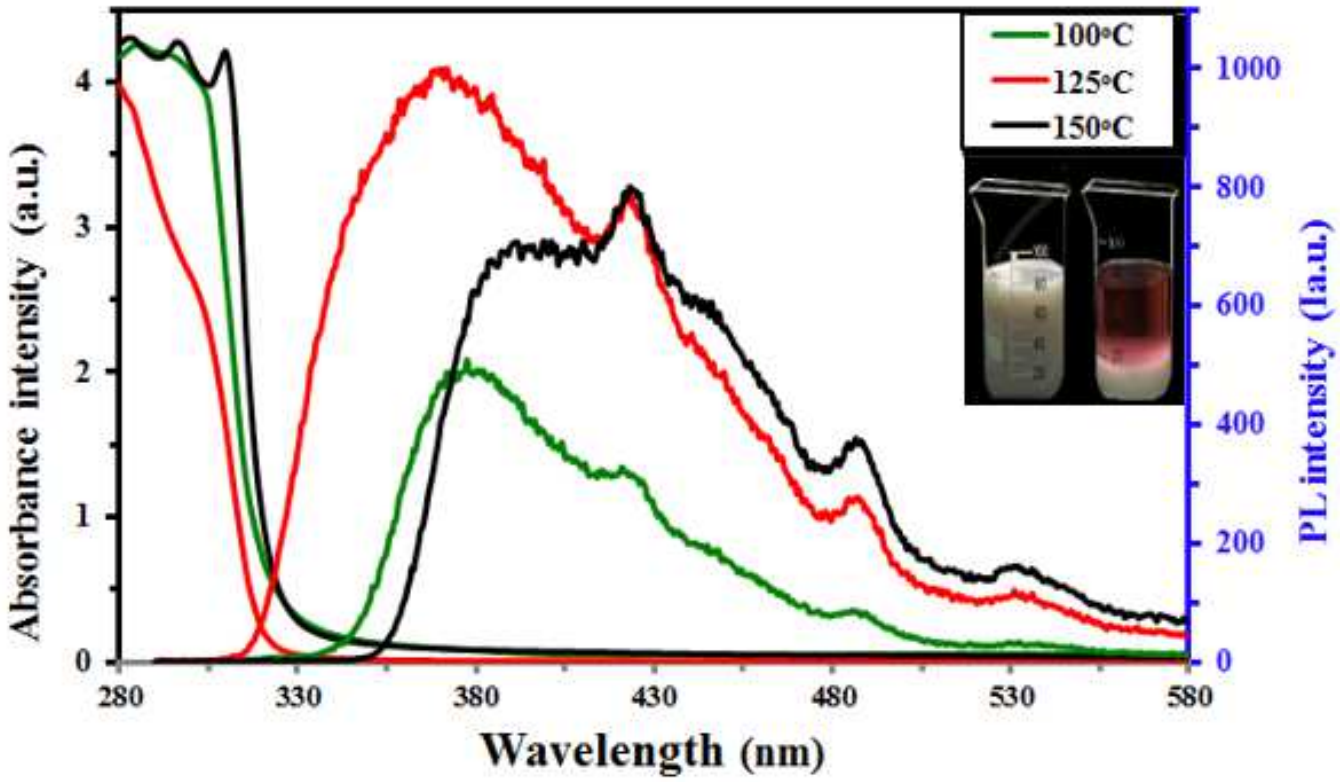

Figure 2. UV-vis absorption and PL emission spectra of MAA capped-ZnS QDs prepared at different temperatures. Inset: Photos of MAA capped-ZnS QDs suspended and precipitated at 150 ^{0}C.

The effect of pH at different pH values of 5, 6.5, 9 and 12 for MAA capped-ZnS QDs synthesis is displayed in Figure 3 It is observed that the absorption and PL spectra are blue shifted by increasing pH due to quantum confinement of the excitons presented in MAA capped-ZnS QDs and decrease of the particle size of the QDs [35]. The band gap values of the prepared MAA capped-ZnS QDs are 3.88 and 3.82 eV at pH of 9 and 6.5, respectively while at 5 and 12 of pH, the precipitation of MAA capped-ZnS QDs is occurred. The pH of the solution has a great effect on the PL intensity. In a slightly acidic medium of pH 6.5 a dissociation of Zn^{2+}–MAA–QDs is happened due to the protonation of the surface binding thiolates groups [33]. However, in a basic medium of pH 9 the PL intensity increases owing to the deprotonation

of thiol groups of the MAA molecule capping agent and the high strength of the covalent bond between thiol and Zn atom at the surface of QDs [36]. In addition, increasing of pH promotes the negative charge of carboxylic acid groups, which assists the dispersion of the formed MAA capped-ZnS QDs [37]. When the pH value is higher than 9 the precipitation of MAA capped-ZnS is occurred due to the formation of $Zn(OH)_2$ onto the QDs surface and this decline of optical characteristics [28].

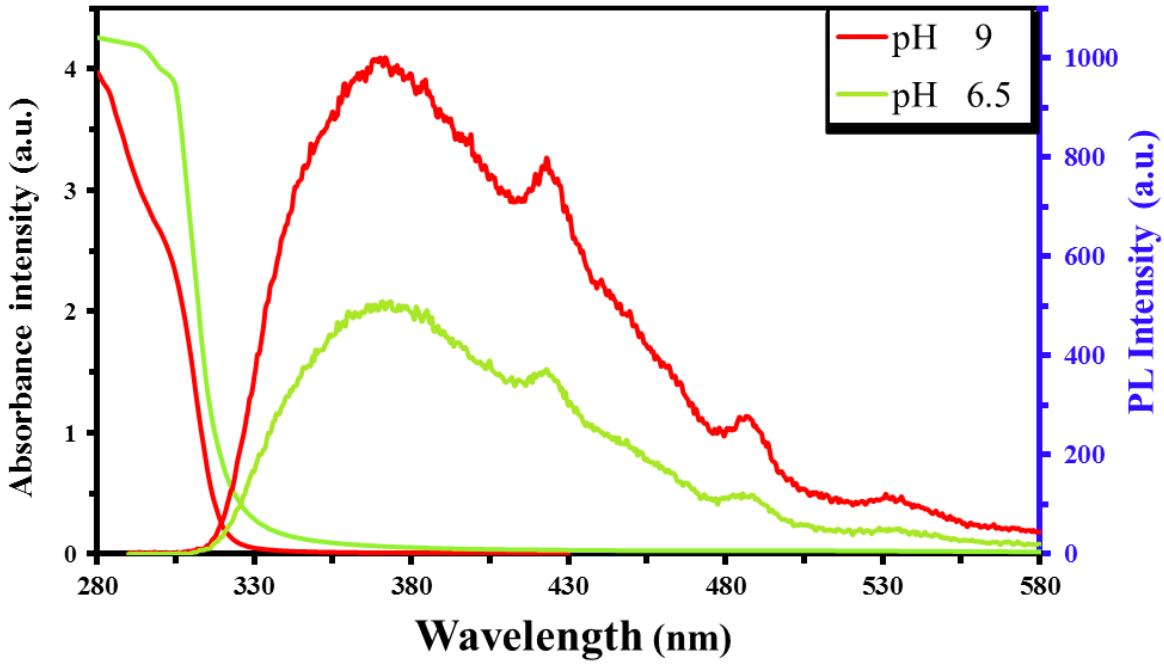

Figure 3. UV-vis absorption and PL emission spectra of MAA capped-ZnS QDs prepared at different pH values

The effect of different Zn^{2+}:S^{2-} molar ratio of 1:2 and 2:1 on the absorbance and emission spectra of MAA capped-ZnS QDs prepared at 125°C and pH of 9 for 2 hrs is presented Figure 4. The absorption spectra of MAA capped-ZnS QDs prepared with 1:2 and 2:1 of Zn^{2+}:S^{2-} molar ratios have two shoulders at 285 and 310 nm, respectively. The absorption shoulder edge positions of the MAA capped-ZnS QDs are found to be red shifted by 25 nm with increasing S^{2-} concentration due to size growth. The band gap values of 1:2 and 2:1 of Zn^{2+}:S^{2-} molar ratios are estimated to be 3.88 and 3.85 eV, respectively. The slightly increase in band gap energy is a result of reduction in the particle size [38]. The increase in the ratio of the S^{2-} indicates a reduction of the particle size. Moreover, the encapsulation of MAA capped-ZnS QDs by excess of Na_2S due to the attractive interaction between S^{2-} anions of Na_2S with the Zn cations of MAA capped-ZnS QDs leads to a decrease in surface defects [37]. It clearly indicates that with the decrease in S^{2-} concentration, the PL intensity is reduced and is accompany by the red shifting of the peak position

from 371 to 380 nm. The PL peak at 380 nm is assigned to transitions involving interstitial Zn^{2+} or S^{2-} atoms. Therefore, decreasing of S^{2-} content, conversely, the increase in Zn^{2+} concentration results in enhancement of S^{2-} vacancies in the synthesized QDs and thus quenches the PL spectra [39]. It can be concluded that the reaction temperature of 125°C at pH of 9 and Zn^{2+}:S^{2-} molar ratio of 1:2 are the optimum conditions for the synthesis of MAA capped-ZnS QDs.

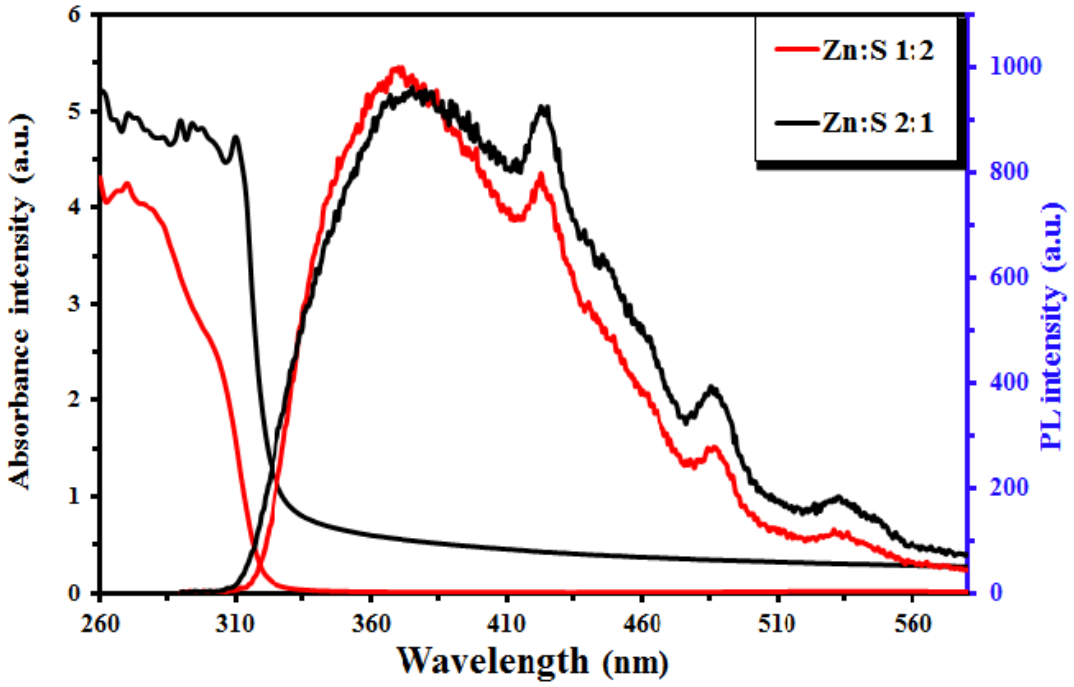

Figure 4. UV-vis absorption and PL spectra of MAA capped-ZnS QDs prepared at different Zn^{2+}:S^{2-} molar ratio of 1:2 and 2:1

The reaction time between the precursors for synthesis of MAA capped-ZnS QDs is a critical parameter and to optimize this time, the effect of different reaction durations on PL is studied as shown in Figure 5. The reaction time of 2 hr has a higher PL intensity than that of reaction time of 1 hr. It is speculated that increasing the emission intensity results from the rearrangement and crystallization of the MAA capped-ZnS QDs by increasing the reaction time, which enhances the quality of the nanocrystals and minimizes the surface defects [40]. After 2 hours, the PL intensity is not only reduced but the suspension is also cloudy observed through the solution and this indicates that the aggregation of QDs or large crystal growth was taking place. It is noted that the precipitation is occurred for the MAA capped-ZnS QDs prepared at 4 and 6 hr reaction time.

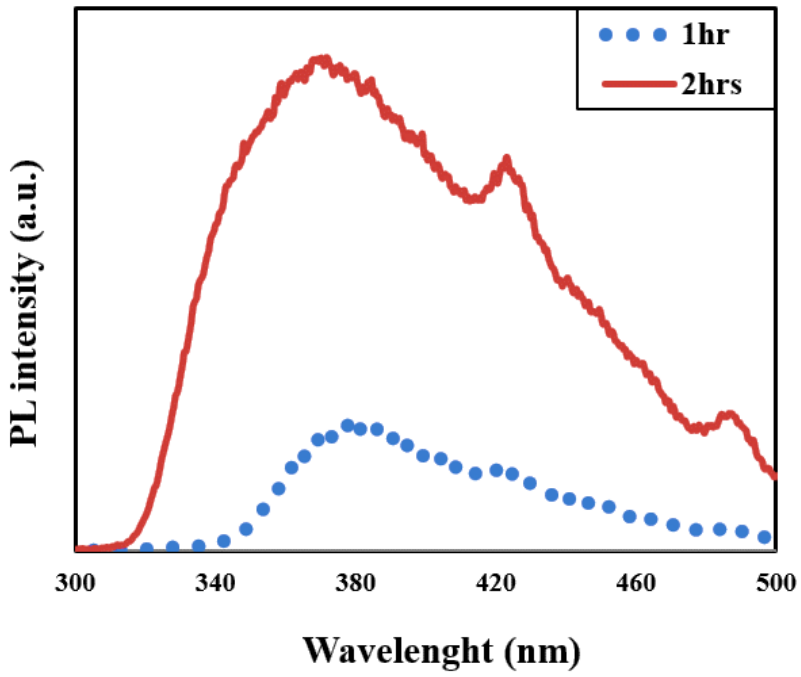

Figure 5. PL spectra of MAA capped-ZnS QDs prepared at different time.

Figure 6a and b displays PL spectra of MAA capped-ZnS QDs prepared at 125°C and pH = 9 for 2 hr using different sources of sulfur such as Na_2S:thiourea and MAA:thiourea molar ratio. It is observed that the 1:1 mixture of Na_2S and thiourea as a sulfur source produces MAA capped-ZnS QDs with high emission PL as presented in Figure 6a. this is due to the excess of sulfur ions reduces the size of MAA capped-ZnS QDs and interacts with the MAA capped-ZnS QDs surface and takes part in interfacial nucleation [6]. On the other hand, MAA capped-ZnS QDs prepared with only Na_2S or thiourea have low emission spectra. This is may be explained by presence of surface defects traps on the surface of the MAA capped-ZnS QDs [27]. MAA:thiourea molar ratio is a key parameter and affects the PL intensities of MAA capped-ZnS QDs [28]. In order to optimize the molar ratio of MAA and thiourea during QDs synthesis, different MAA:thiourea molar ratios are used and the PL intensity is measured. It is noted that 1:1 ratio of MAA:thiourea has the highest PL intensity due to the synthesis of completely MAA capped-ZnS QDs as shown in Figure 6b. Three luminance peaks at 371, 423 and 486 nm are appeared and for MAA capped-ZnS QDs there are deep vacancy states lies in the gap arising from interstitial atoms [41]. Therefore, it is concluded that the two peaks at 423 and 486 nm are attributed to the interstitial sulfur and zinc, respectively and the peak at 371 nm is due to Zn vacancies [42]. The proposed schematic energy level diagram of MAA capped-ZnS QDs with the three types of point defects is depicted in Figure 6c. Because the S^{2-} ions are larger than the Zn ions, interstitial sulfur induces more strain to the lattice. Electron levels

originating from this defect have smaller binding energies due to such strain. Therefore, interstitial S states should be located closer to the valence band edge than interstitial Zn states to the conduction band edge [41]. For MAA:thiourea molar ratio of 2:1 or 1:2 there is a decrease in PL and this can be explained based on the interference and crowding of the excess of MAA or thiourea on QDs surfaces. For MAA:thiourea of 2:1 molar ratio, it is observed that there is a red shift of the peak position from 371 nm to 376 nm due to formation of large size MAA capped-ZnS QDs as a result of large number of ligand molecules which crosslink with each other on the surface on MAA capped-ZnS QDs [38]. An excess amount of thiourea in solution of MAA:thiourea with 1:2 molar ratio promotes the hydrolysis of thiourea, and therefore, a higher sulfide S^{2-} content in the reaction medium accelerates the growth of the QDs. This leads to the coarse surface and poor optical properties [35]. On the other hand, low PL of MAA capped-ZnS QDs prepared with only MAA or thiourea results in incomplete capped of MAA capped-ZnS QDs. MAA:thiourea molar ratio of 1:1 is the optimum for preparing MAA capped-ZnS QDs. This indicates that thiourea has a capping agent role in the synthesis of MAA capped-ZnS QDs [2]. From previous results, it can be concluded that the optimum conditions for preparing MAA capped-ZnS QDs with high PL signals are 125°C, pH of 9, 1:2 of Zn^{2+}:S^{2-} molar ratio and 1:1 of MAA: thiourea molar ratio with using identical mixture of Na_2S and thiourea as a sulfur source.

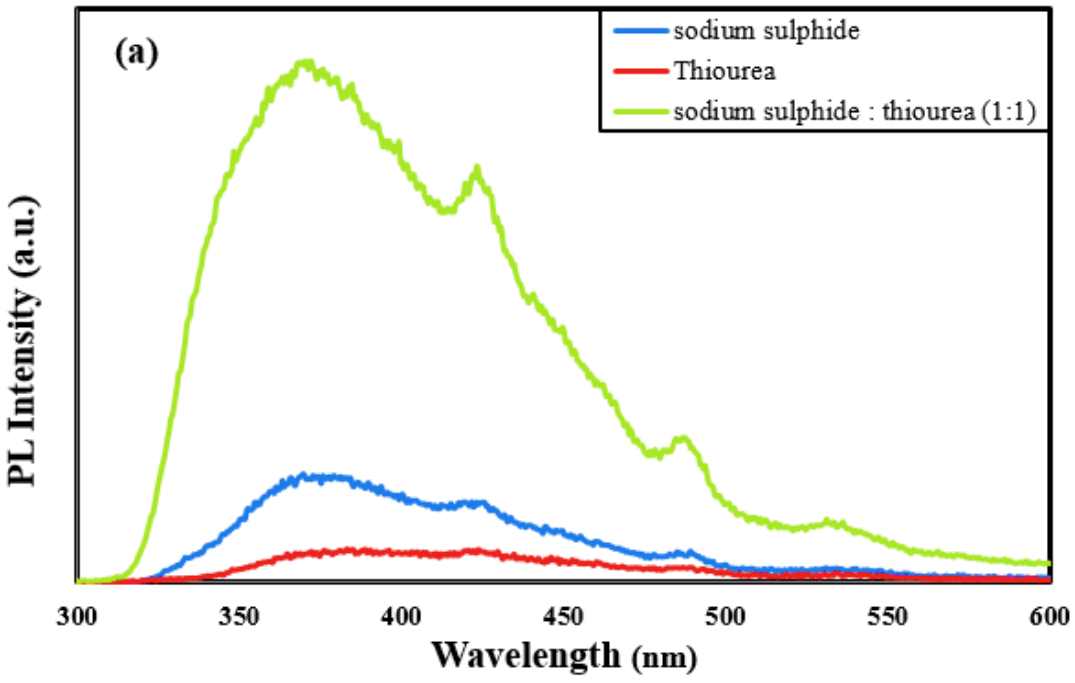

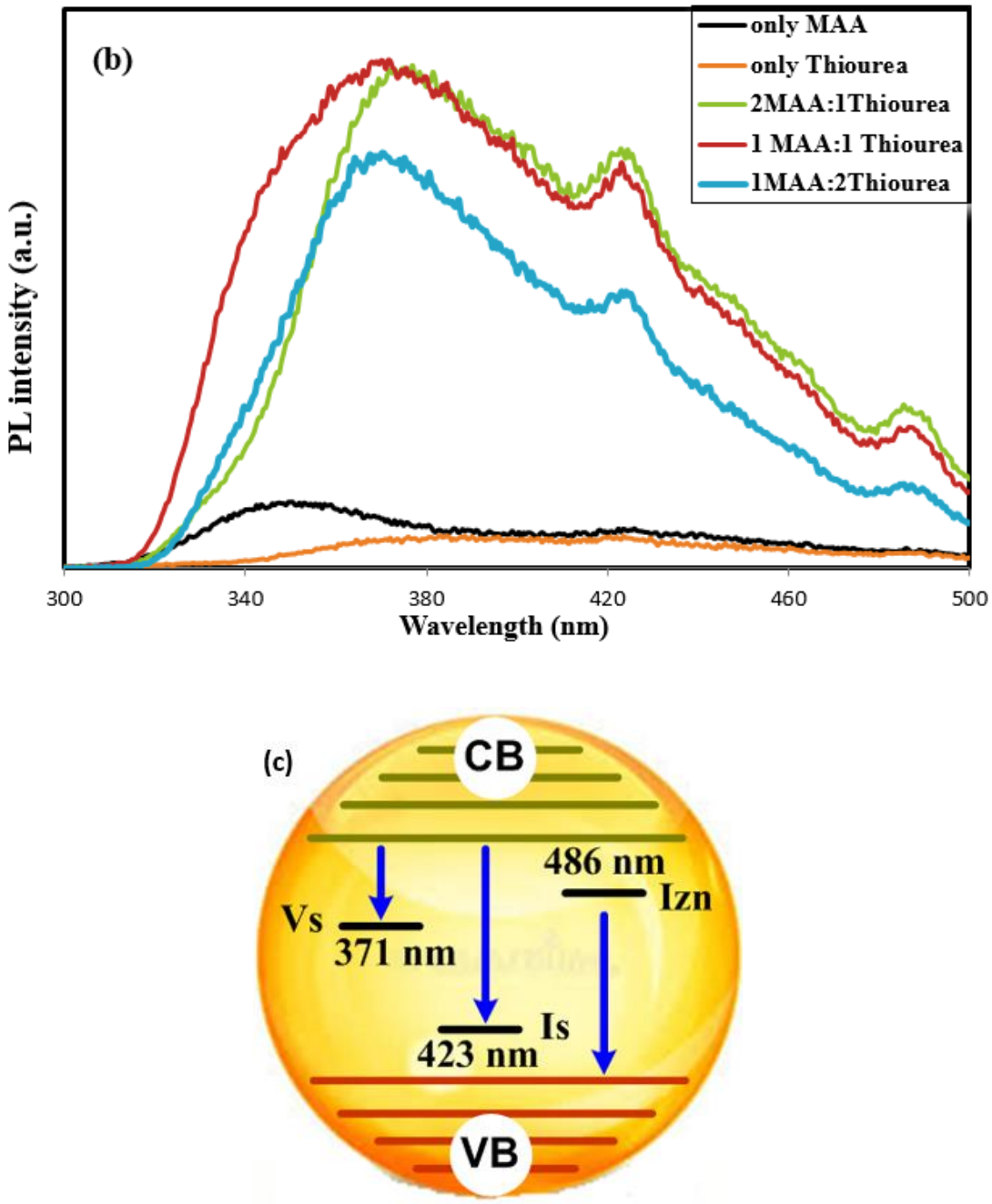

Figure 6. PL emission spectra of MAA capped-ZnS QDs prepared at different (a) source of sulfur, (b) molar ratios of MAA:thiourea, (c) Schematic energy level diagram of point defects in MAA capped-ZnS QDs. where: I_S = interstitial sulfur, I_{Zn}= interstitial zinc and V_{Zn}= zinc vacancy,

The role of capping agent is primarily as a stabilizing agent, providing colloidal stability, stopping uncontrolled growth and agglomeration [8]. Using thiol capping agent is an important, where the energy levels of the thiol inhibit hole trapping and the resulting QDs are extremely luminescent without the need

for further inorganic shells to protect QDs from oxidizing [4]. Photostability rate of the MAA capped-ZnS QDs presented in equation (1) is a significant parameter for detection applications, where A_t and A_0 is the area under the PL curve at certain month and at time zero directly after preparation. The PL of the MAA capped-ZnS QD was tested after storing on shelf for 14 months without further protection in the ambient conditions as shown in Figure 7. The PL intensity of MAA capped-ZnS QDs retains about 12% of its original value after 14 months without any peak shift as shown in inset Figure 7. This promotes the high photostability of MAA capped-ZnS QDs.

$$\textbf{photostability} = \left|\frac{\mathbf{A_t - A_0}}{\mathbf{A_0}}\right| \times \mathbf{100} \quad (1)$$

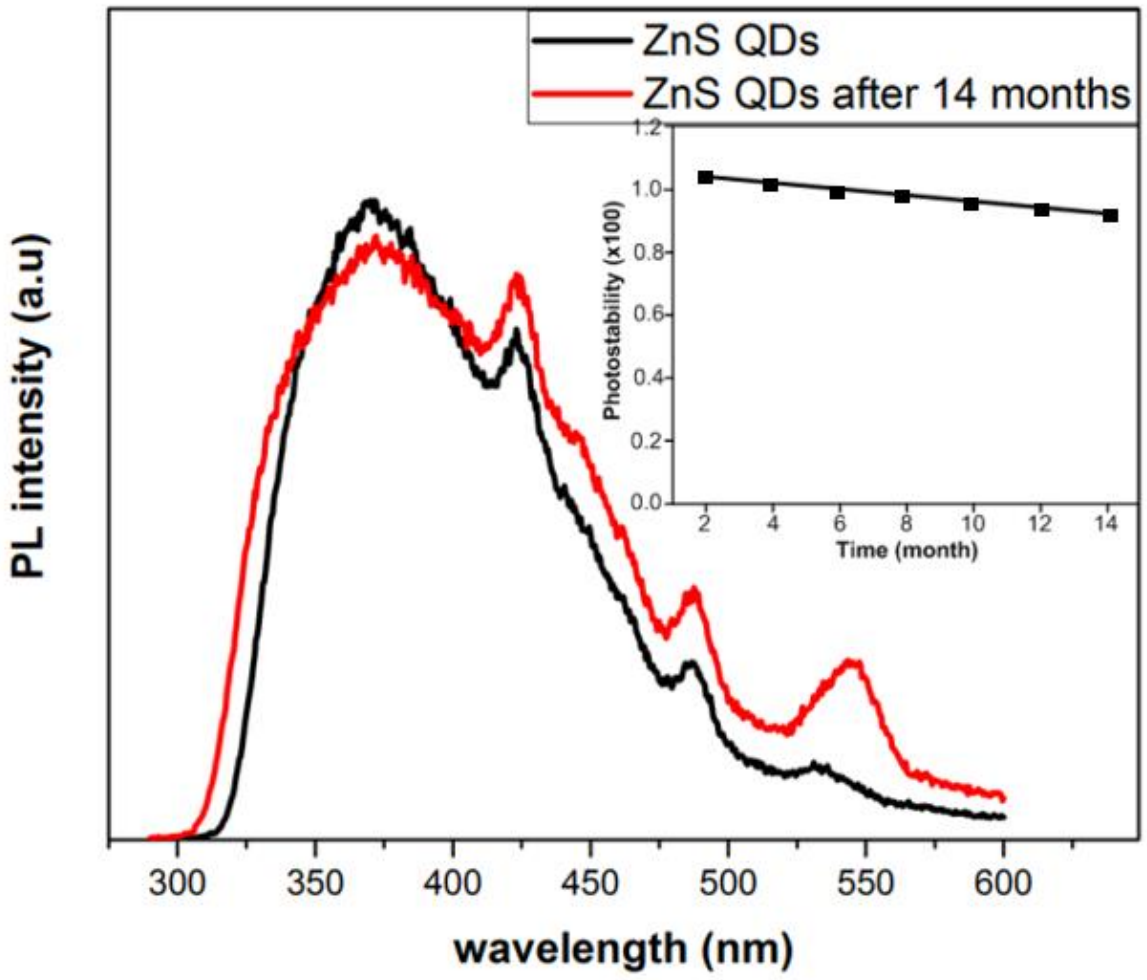

Figure 7. PL photostability of the MAA capped-ZnS QDs after 14 months, inset Photostability rate (×100) of MAA capped-ZnS QDs versus time.

3.2 Structural, morphological, and elemental Analysis of MAA capped-ZnS Quantum Dots

The MAA capped-ZnS QDs samples prepared at optimum condition are analyzed by XRD, HRTEM, and EDX. The XRD pattern spectrum depicted in Figure 8 shows a various diffraction peaks at 2θ values of 28.6°, 47.6° and 56.4° corresponding to the diffraction planes (111), (220) and (311), respectively. The XRD of the MAA capped-ZnS QDs correlates and agrees with the JCPDS number 05-0566 of cubic zinc blend phase structure of ZnS [17]. The broadening peaks of the XRD pattern of MAA capped-ZnS QDs are observed due to their small crystalizes size and this confirms that pure cubic ZnS has nano-crystallites [27]. XRD pattern also confirms that MAA capped-ZnS QDs contains pure cubic ZnS without any diffraction peaks of impurities detected, [19,37,43].

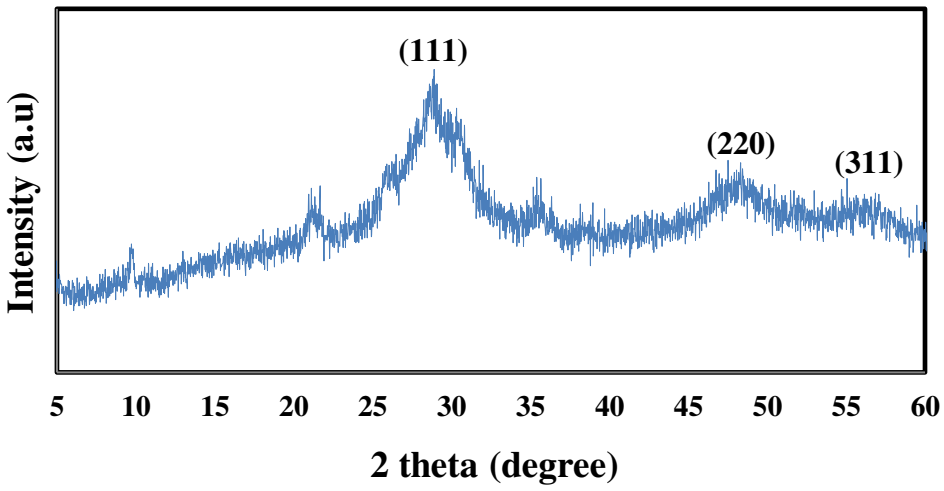

Figure 8. XRD pattern of MAA capped-ZnS QDs.

Figure 9 displays HRTEM images of MAA capped-ZnS QDs with a cubic structure and an average size of 8.8 nm. The presence of the lattice plan on the HRTEM images of the particles indicates that MAA capped-ZnS QDs are highly crystalline. The inset HRTEM images represnted these lattice space with a spacing of 0.35 nm and this is in agreement with the spacing of cubic ZnS (111) planes [19,21,38]. The

inset of Figure 9 illustrates the selected area electron diffraction (SAED) patterns of the MAA capped-ZnS QDs obtained from bright field HRTEM image and confirms the crystalline nature of the MAA capped-ZnS QDs. Many rings are detected, among them the strongest three rings correspond to the (111), (220) and (311) planes of the cubic phase of ZnS [38].

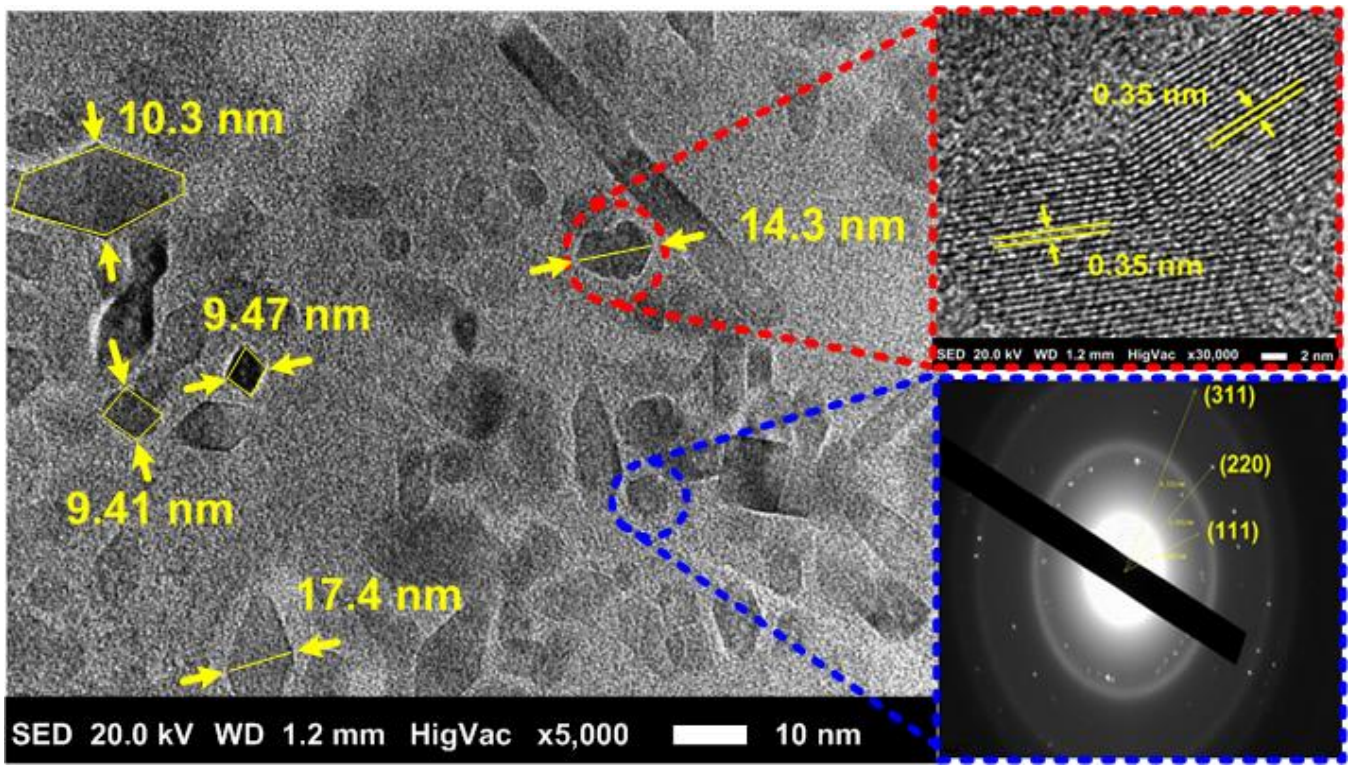

Figure 9. HRTEM images of MAA capped-ZnS QDs with high magnification image and SAED image were inserted as inset.

The chemical composition and stoichiometry of the synthesis MAA capped-ZnS QDs sample is investigated by EDX as shown in Figure 10. It is confirmed that the presence of Zn, S, C, Cu and O elements appears a successful synthesis of MAA capped-ZnS QDs. Cu comes from the grid used for HRTEM analysis, whereas O and C results from the capping agent of the sample [36]. The S element is existed from the source of sodium sulphide during the preparation process of MAA capped-ZnS QDs [4].

The weight and atomic percentages of the Zn^{2+}:S^{2-} elements in the MAA capped-ZnS QDs are determined 2.42 and 1.18, respectively as shown in the inset of Figure 10.

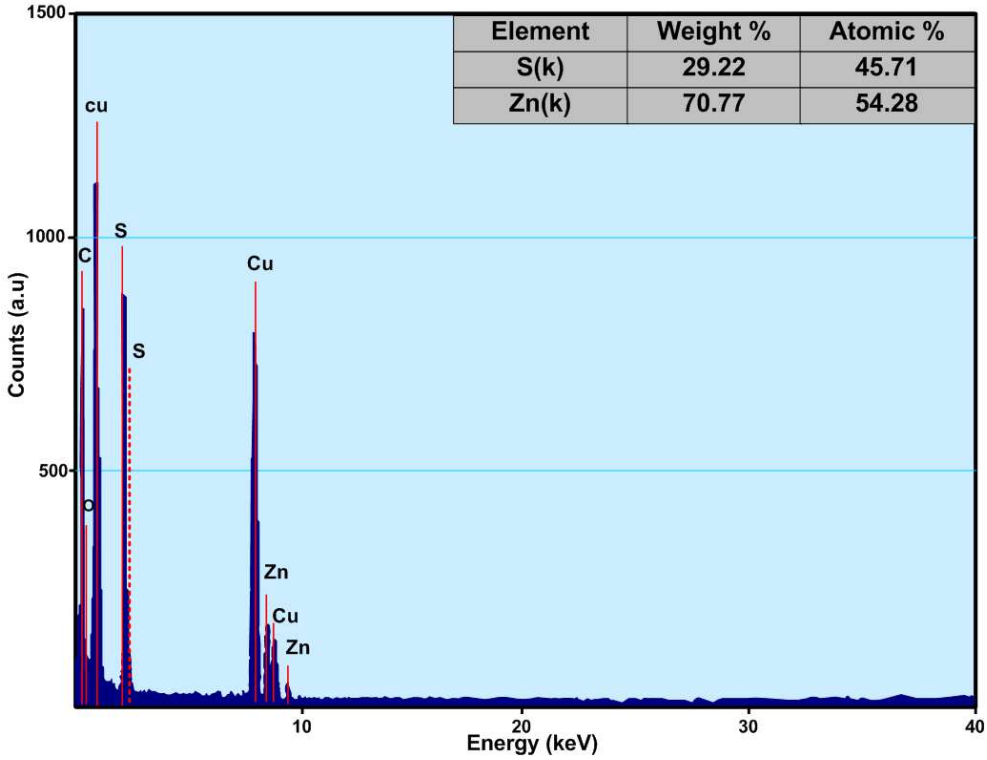

Figure 10. EDX of MAA capped-ZnS QDs. inset table declare the weight and atomic percentages of the Zn^{2+}:S^{2-} elements

3.6 Detection of free chlorine concentrations by MAA capped-ZnS QDs

PL emission curves at different emission wavelengths in the range of 300 to 500 nm are plotted versus chlorine concentration in the range of 1 to 35 ppm as presented in Figure 11. The PL emission peak intensity of MAA capped-ZnS QDs/NaClO system is inversely proportional to the injected free Cl_2 concertation and the luminosity is disappeared above 35 ppm concentration of Cl_2 ions. This is consistent with the reported data by by Callan et al and Gunnlaugsson et al [44, 45, 9, 10]. The MAA capped-ZnS QDs/NaClO system detection for chlorine can be measured by oxidation of NaClO to generate Cl_2 and ClO^- ions in aqueous solution. The PL spectra of MAA capped-ZnS QDs/NaClO system have a board emission peak centered at 358 nm with a small shoulder reported at 440 nm. Higher concentrations of NaClO than 35 ppm are not desired due to the quenching effect of MAA capped-ZnS QDs resulted from the collision of MAA capped-ZnS QDs with Cl_2 and ClO^- at high concentration. The Cl_2 detection

mechanism of the MAA capped-ZnS QDs/NaClO system is schematically presented in Figure 12. The PL intensity of the MAA capped-ZnS QDs/NaClO system is quenched due to the reduction of hypochlorite ion to chloride ion presented in the system by the gain of excited electron from the sulphur vacancy of MAA capped-ZnS QDs [10]. The PL vs. Cl_2 relationship is consistent with the Förster resonance energy transfer (FRET) mechanism of quenching such that MAA capped-ZnS QDs served as a FRET donor and the conjugated-thiourea served as the FRET receptor as shown in the quenched emission pathway 1 in Figure 12 [44]. Therefore, the electron transfer from the MAA capped-ZnS QDs to NaClO is happened and NaClO could inject the holes into the MAA capped ZnS QDs valance band (VB) and convert MAA capped ZnS QDs to oxidized-state MAA capped ZnS QDs (MAA capped ZnS $QDs^{\bullet+}$). On the other hand, in pathway 2, the MAA capped-ZnS QDs act as electron donors in the redox reaction could also transfer the electrons to the conduction band (CB) of the oxidized-state MAA capped-ZnS $QDs^{\bullet+}$ and an active oxygen free radical (•OH and $O_2^{\bullet-}$) are formed. Meanwhile, the generated excited-state MAA capped-ZnS $QDs^{\bullet+}$ returns to the VB and releases photons [46].

The PL intensity of MAA capped-ZnS QDs and the concentration of Cl_2 can be examined Stern–Volmer (SV) relation as follows [27,39,40]:

$$\frac{F_0}{F} = k_{sv}[Q] + 1 \qquad (2)$$

where F_0 and F are the peak intensities of MAA capped-ZnS QDs before and after of addition of quencher [Q] and Ksv stands to the Stern-Volmer constant. The calibration curve of MAA capped-ZnS QDs displayed in the inset of Figure 11 follows the equation of Stern-Volmer with F_0/F as a function of Cl_2 concentration in the range of 1–35 ppm. The calibration equation curve of $Y = 0.0696\ X + 0.7665$ ($Y=F_0/F$, X=concentration) shows a good linearity with a correlation coefficient $R^2 = 0.9782$. The estimated sensitivity (Ksv) is found to be 31.43×10^{-2} ppm^{-1} and limit of detection (LOD) is calculated to be 3.6 mg/L.

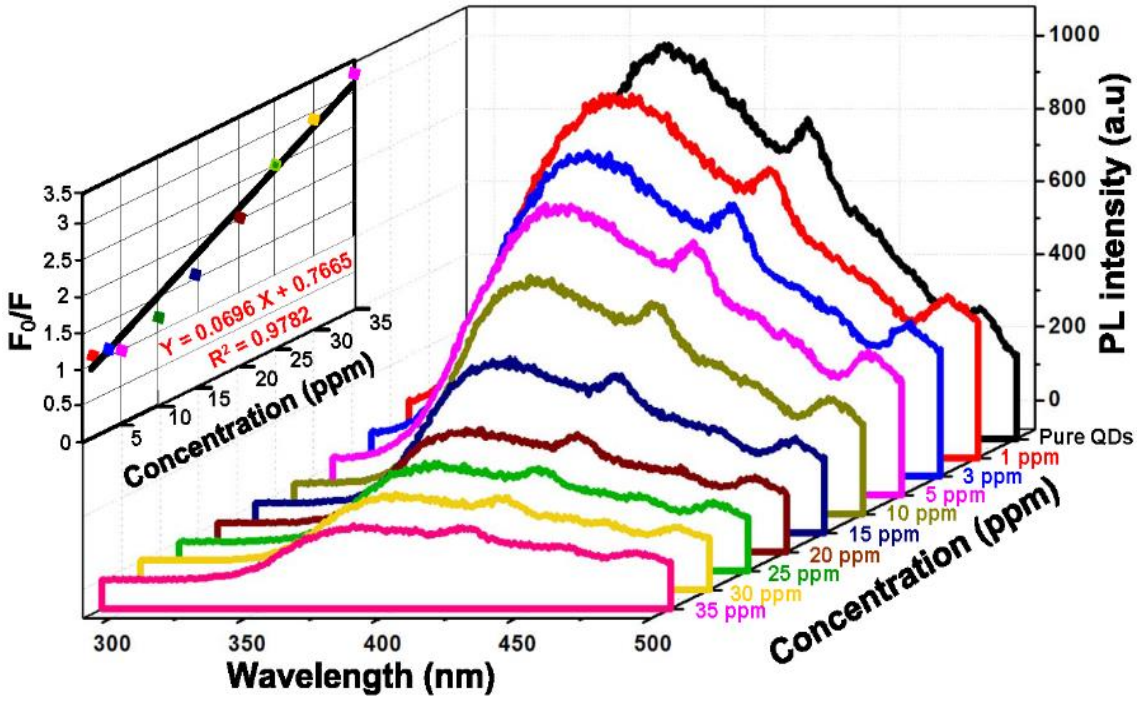

Figure 11. Stern-Volmer relationship between PL intensity of MAA capped-ZnS QDs and concentrations of free chlorine.

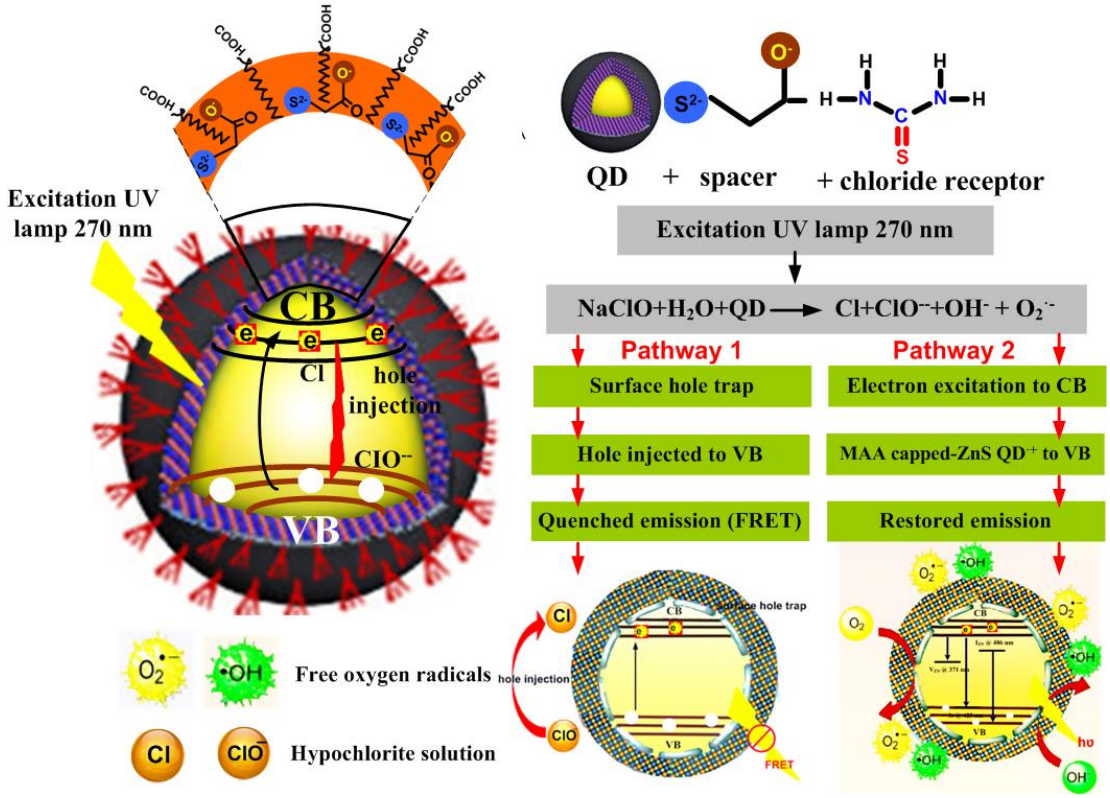

Figure 12. Schematic illustration of Cl_2 mechanism of MAA capped-ZnS QDs/NaClO system

4. Conclusion

A highly luminesces photostable MAA capped-ZnS QDs in aqueous solution in the presence of MAA as a capping agent were prepared using the hydrothermal method to be used for Cl_2 sensing application. The estimated energy band gab of MAA capped-ZnS QDs from Tauc's plot was 3.88 eV. PL spectra of the MAA capped-ZnS QDs revealed three emission peaks at 371 nm attributed to V_{Zn} and 423 and 486 nm were caused due to transitions involving I_S and I_{Zn}, respectively. The XRD and HRTEM confirmed that MAA capped-ZnS QDs have a cubic structure. The sensing effect of MAA capped-ZnS QDs was used to detect small free Cl_2 concentration in the range from 1 to 35 ppm and exhibited a good linearity with $R^2 = 0.9782$. The sensitivity and LOD of MAA capped-ZnS QDs as Cl_2 sensor were found to 31.43×10^{-2} ppm^{-1} and 3.6 mg/L, respectively.

Declaration

Tosson Shaala: Preparation and characterization. Jehan El Nady: Supervision, Conceptualization, Writing - original draft, preparation. Shaker Ebrahim and Moataz Soliman: Supervision, Conceptualization, Writing – review & editing. A.M. Elshaer: preparation, conceptualization, Measurements.

References

[1] Q. Li, L. Dong, X. Wang, L. Huang, H. Xie, C. Xiong, Scr. Mater. **66**, 646 (2012). https://doi.org/10.1016/j.apsusc.2014.07.135

[2] R. Hamid, M. Farsi, Mater. Sci. Semicond. Process. **48**, 14 (2016). https://doi.org/10.1016/j.mssp.2016.02.021

[3] M. Shehab, S. Ebrahim, M. Soliman, J. Lumin. **184**, 110 (2017). https://doi.org/10.1016/j.jlumin.2016.12.006

[4] K. Amer, A. M. Elshaer, M. Anas, S. Ebrahim, J. Mater. Sci.: Mater. **30**, 391 (2019). https://doi.org/10.1007/s10854-018-0303-7

[5] E. Goharshadi, S. Sajjadi, R. Mehrkhah, P. Nancarrow, Chem. Eng. J. **209**, 113 (2012). https://doi.org/10.1016/j.cej.2012.07.131

[6] L. Waldron, R. Burke, A. Preske, T. Krauss, J. Zawodny, M. C. Gupta, Appl. Opt. **56,** 1982 (2017). https://doi.org/10.1364/AO.56.001982

[7] X. Xiong, Y. Tang, L. Zhang, S. Zhao, Talanta. **132,** 790 (2015). https://doi.org/10.1016/j.talanta.2014.10.022

[8] C. Neumann, C. Volk, S. Engels, C. Stampfer, Nanotechnology **24,** 444001 (2013). https://doi.org/10.1088/0957-4484/24/44/444001

[9] T. Hallaj, M. Amjadi, J. Manzoori, R. Shokri, Microchim Acta. **182**, 789 (2015). https://doi.org/10.1007/s00604-014-1389-0

[10] K. Singh, S. Mehta, Analyst. **141**, 2487 (2016). https://doi.org/10.1039/c5an02599k

[11] M. Murata, T. Ivandini, M. Shibata, S. Nomura, A. Fujishima, Y. Einaga, J. Electroanal. Chem. **612**, 29 (2008). https://doi.org/10.1016/j.jelechem.2007.09.006

[12] S. Kishioka, T. Kosugi, A.Yamada, Electroanalysis. **17,** 724 (2005). https://doi.org/10.1002/elan.200403135

[13] C. Kang, D. Xi, S. Zhou, Z. Jiang, Talanta. **68**, 974 (2006). https://doi.org/10.1016/j.talanta.2005.06.066

[14] Y. Yan, S. Wang, Z. Liu, H. Wang, D. Huang, Anal. Chem. **82,** 9775 (2010). https://doi.org/10.1021/ac101929q

[15] Y. Dong, G. Li, N. Zhou, R. Wang, Y. Chi, G. Chen, Anal. Chem. **84**, 8378 (2012). https://doi.org/10.1021/ac301945z

[16] M. Iqbal, S. Iqbal, J. Lumin. **134**, 739 (2013). https://doi.org/10.1016/j.jlumin.2012.07.001

[17] A. Jothi, G. Amish, R. Joshi, C. Vijay, A. Muthuvinayagam, P. Sagayaraj, Mater. Chem. Phys. **138**, 186 (2013). https://doi.org/10.1016/j.matchemphys.2012.11.042

[18] H. Rajabi, M. Farsi, J. Mol, Catal. A. Chem. **399,** 53 (2015). https://doi.org/10.1016/j.molcata.2015.01.029

[19] C. Liu, Y. Ji, T. Tan, J. Alloys Compd. **570**, 23 (2013). https://doi.org/10.1016/j.jallcom.2013.03.118

[20] L. Sun, C. Yan, C. Liu, C. Liao, L. Dan, J. Yu, J. Alloys Compd. **275,** 234 (1998). https://doi.org/10.1016/s0925-8388(98)00310-7

[21] M. Ali, D. Zayed, W. Ramadan, O. Kamel, M. Shehab, S. Ebrahim, Int. Nano Lett. **9,** 61 (2019). https://doi.org/10.1007/s40089-018-0262-2

[22] M. Iqbal, S. Iqbal, J. Lumin. **134**, 739 (2013). https://doi.org/10.1016/j.jlumin.2012.07.001

[23] A. Mansour, M. Abdo, F. Abdel Maged, G. Agag, J. Inorg. Organomet. Polym. Mater. **1**, 1 (2021). https://doi.org/10.1007/s10904-021-01884-8

[24] O. Daramola, X. Noundou, C. Nkanga, P. Tseki, R. Krause, J. Fluoresc. **30**, 557 (2020). https://doi.org/10.1007/s10895-020-02526-x

[25] O. Acar, W. Shih, W. Shih, Chem. Phys. Lett. **754,** 137696 (2020). https://doi.org/10.1016/j.cplett.2020.137696

[26] D. Ramírez-Herrera, E. Rodríguez-Velázquez, M. Alatorre-Meda, F. Paraguay-Delgado, A. Tirado-Guízar, P. Taboada, G. Pina-Luis, Nanomaterials. **8,** 231 (2018). https://doi.org/10.3390/nano8040231

[27] M. Mostafa, J. ElNady, S. Ebrahim, A. M. Elshaer, Opt. Mater. **112,** 110732 (2021). https://doi.org/10.1016/j.optmat.2020.110732

[28] M. Yaraki, M. Ahmadieh, A. Mogharei, M. Tahriri, D. Vashaee, L. Tayebi, J. Alloys Compd. **690**, 749 (2017). https://doi.org/10.1016/j.jallcom.2016.08.158

[29] S. Wageha, Z. Su Linga, X. Xu-Rong, J. Cryst. Growth. **255**, 332 (2003). https://doi.org/10.1016/S0022-0248(03)01258-2

[30] A. Magdy, J. ElNady, S. Ebrahim, M. Soliman, Opt. Mater. **86**, 545 (2018). https://doi.org/10.1016/j.optmat.2018.10.058

[31] H. Rajabi, M. Farsi, Mater. Sci. Semicond. Process. **48**, 14 (2016). https://doi.org/10.1016/j.mssp.2016.02.021

[32] J. Oliveira, R. Brito-Pereira, B. Gonçalves, L. Etxebarria, S. Lanceros-Mendez, Org. Electron. **66**, 216 (2019). https://doi.org/10.1016/j.orgel.2018.12.028

[33] D. Zhou, H. Zhang, Small. **9** 3195-3197 (2013). https://doi.org/10.1002/smll.201201060

[34] J. Guo, W. Yang, C. Wang, J. Phys. Chem. **109**, 17467 (2005). https://doi.org/10.1021/jp044770z

[35] A. Emamdoust, S. Shayesteh, M. Marandi, J. Phys. **80**, 713 (2013). https://doi.org/10.1007/s12043-013-0512-9

[36] M. Koneswaran, R. Narayanaswamy, Microchim Acta. **178**, 171 (2012). https://doi.org/10.1007/s00604-012-0819-0

[37] S. Ebrahim, M. Labeb, T. Abdel-Fattah, M. Soliman, J. Lumin. **182**, 154 (2017). https://doi.org/10.1016/j.jlumin.2016.09.038

[38] M. Mrad, T. Chaabane, H. Rinnert, B. Lavinia, J. Jasniewski, G. Medjahdi, R. Schneider, Inorg. Chem. **59**, 6220 (2020). https://doi.org/10.1021/acs.inorgchem.0c00347

[39] G. Ghosh, M. Naskar, A. Patra, M. Chatterjee, Opt. Mater. **28,** 1047 (2006). https://doi.org/10.1016/j.optmat.2005.06.003

[40] G. Lan, Y. Lin, Y. Huanga, H. Chang, J. Mater. Chem. **17**, 2661 (2007). https://doi.org/10.1039/B702469J

[41] D. Denzler, M. Olschewski, K. Sattler, J. Appl. Phys. **84,** 2841 (1998). https://doi.org/10.1063/1.368425

[42] A. Shaikh, P. Sonawane, J. Appl. Phys. **3**, 99 (2016). https://doi.org/10.9790/4861-08030299104

[43] K. Ghoderao, S. Jamble, J. Sawant, R. Kale, Mater. Res. Express. **4,** 025 (2017). https://doi.org/10.1088/2053-1591/aa5c00

[44] W. Yuchi, H. Mao, B. Wong, Nanotechnology. **21**, 055101 (2009). https://doi.org/10.1088/0957-4484/21/5/055101

[45] D. Wu, C. Adam, T. Gunnlaugsson, U. Enginy, J. Yoon, T. James, Chem. Soc. Rev. **46,** 7105 (2017). https://doi.org/10.1039/c7cs00240h

[46] Y. Tang, H. Song, Y. Su, Y. Lv, Anal. Chem. **85**, 11876 (2013). https://doi.org/10.1021/ac403517u

Figures

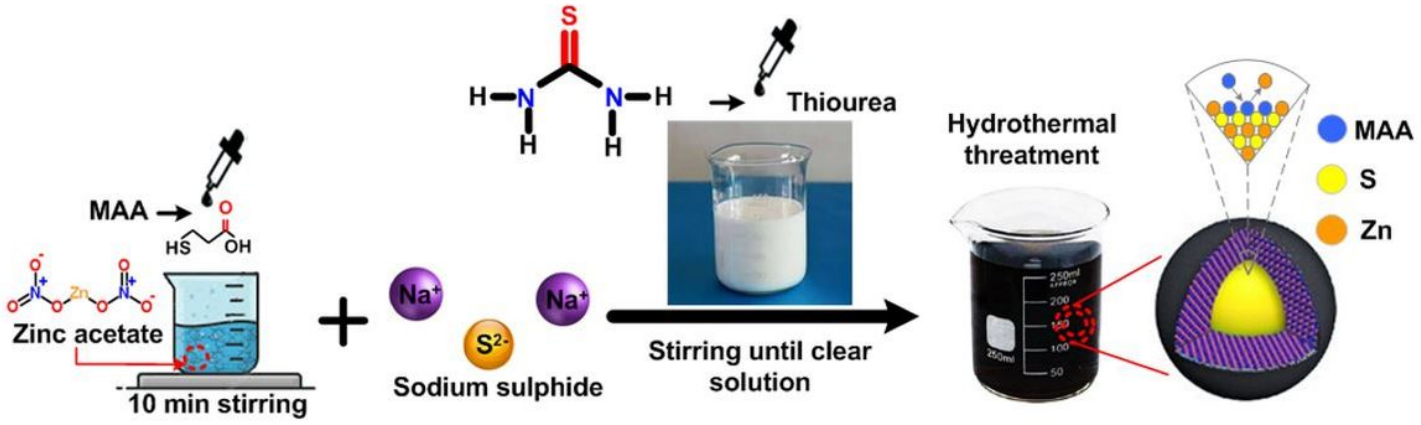

Figure 1

preparation steps diagram of MAA capped-ZnS QDs.

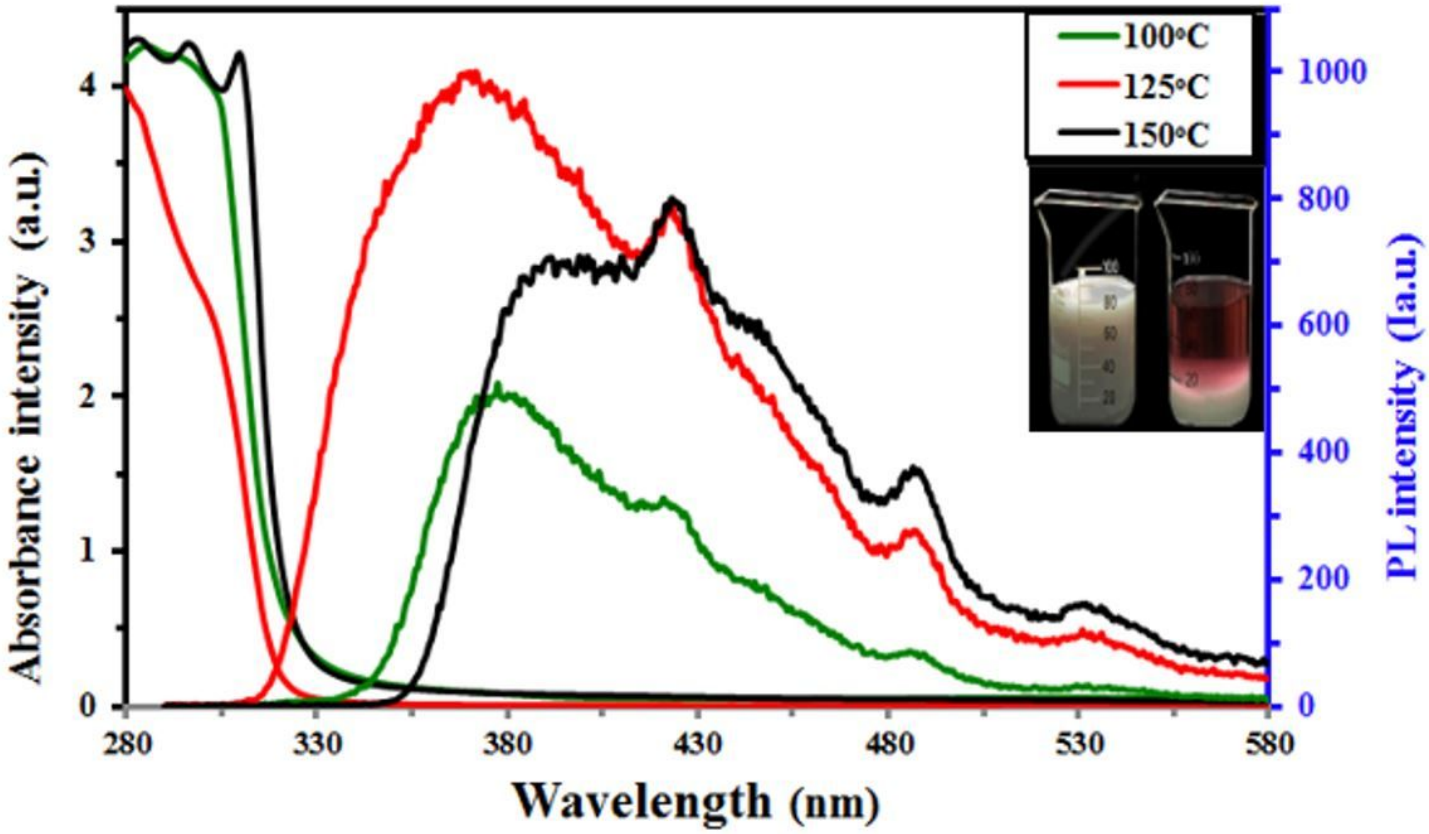

Figure 2

UV-vis absorption and PL emission spectra of MAA capped-ZnS QDs prepared at different temperatures. Inset: Photos of MAA capped-ZnS QDs suspended and precipitated at 150 0C.

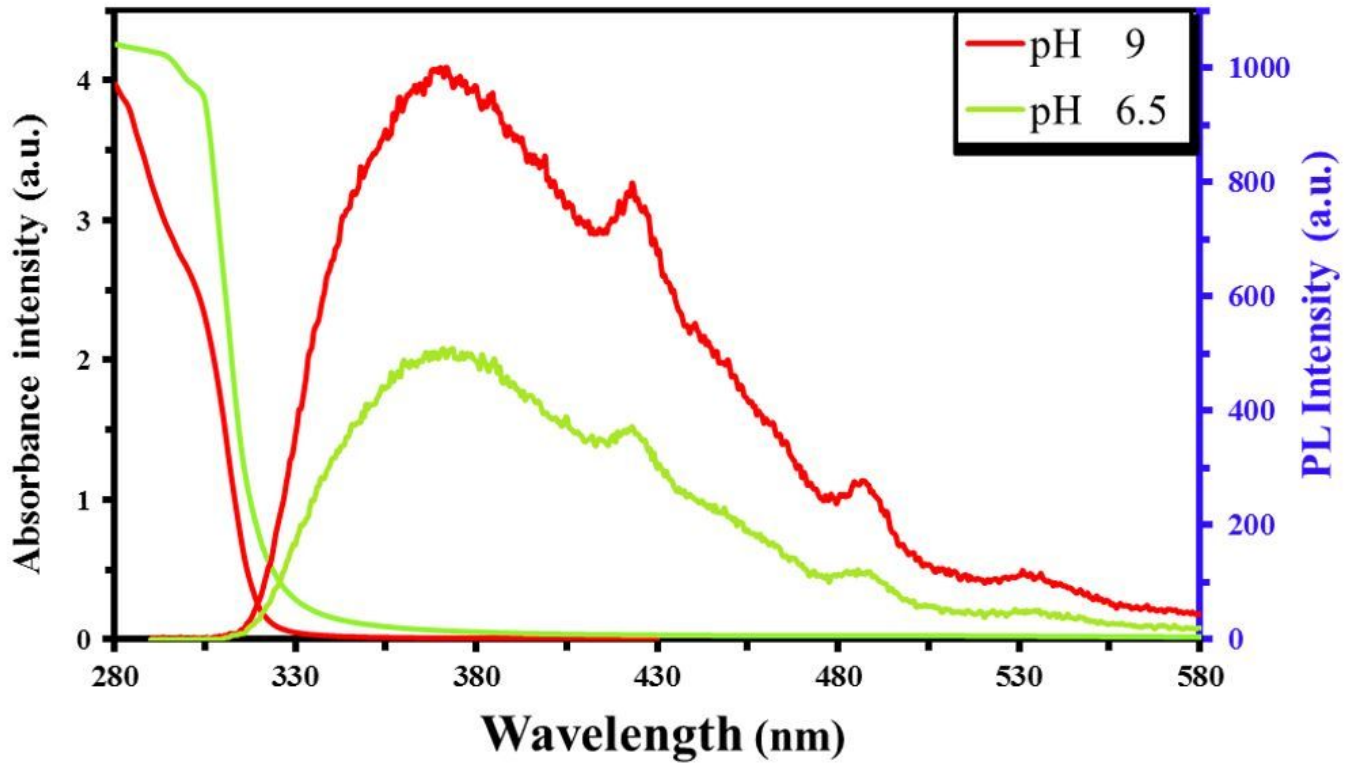

Figure 3

UV-vis absorption and PL emission spectra of MAA capped-ZnS QDs prepared at different pH values

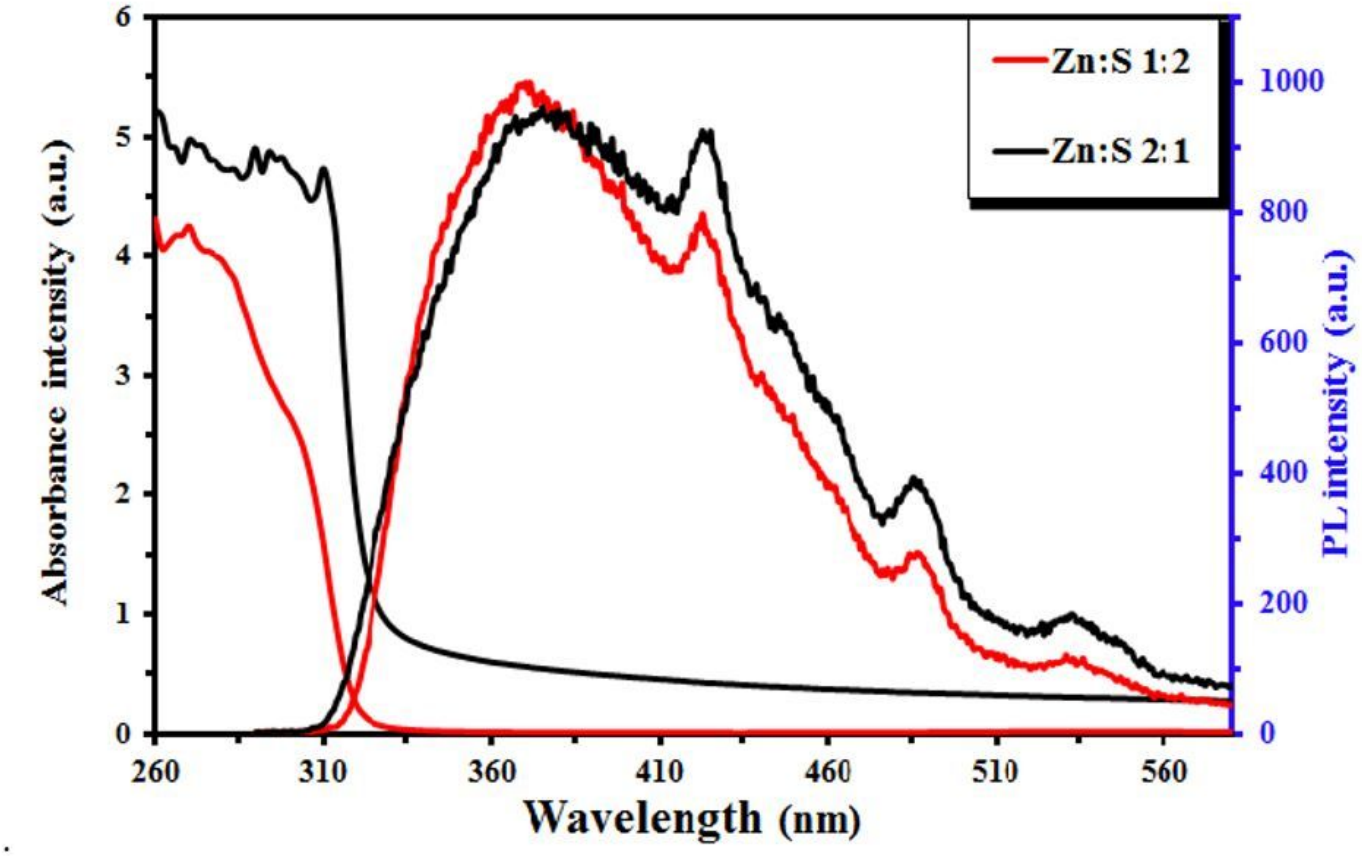

Figure 4

UV-vis absorption and PL spectra of MAA capped-ZnS QDs prepared at different Zn2+:S2- molar ratio of 1:2 and 2:1

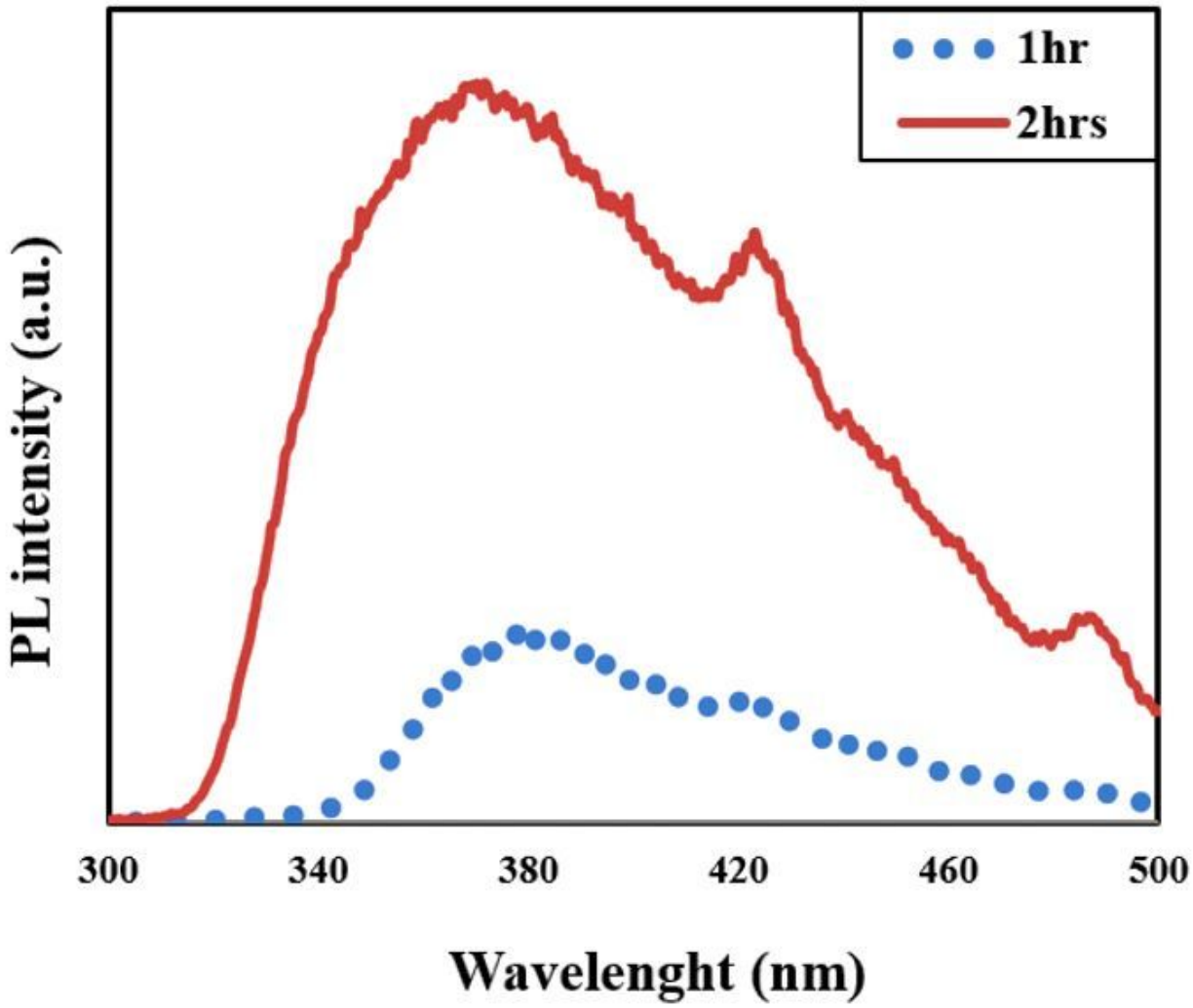

Figure 5

PL spectra of MAA capped-ZnS QDs prepared at different time.

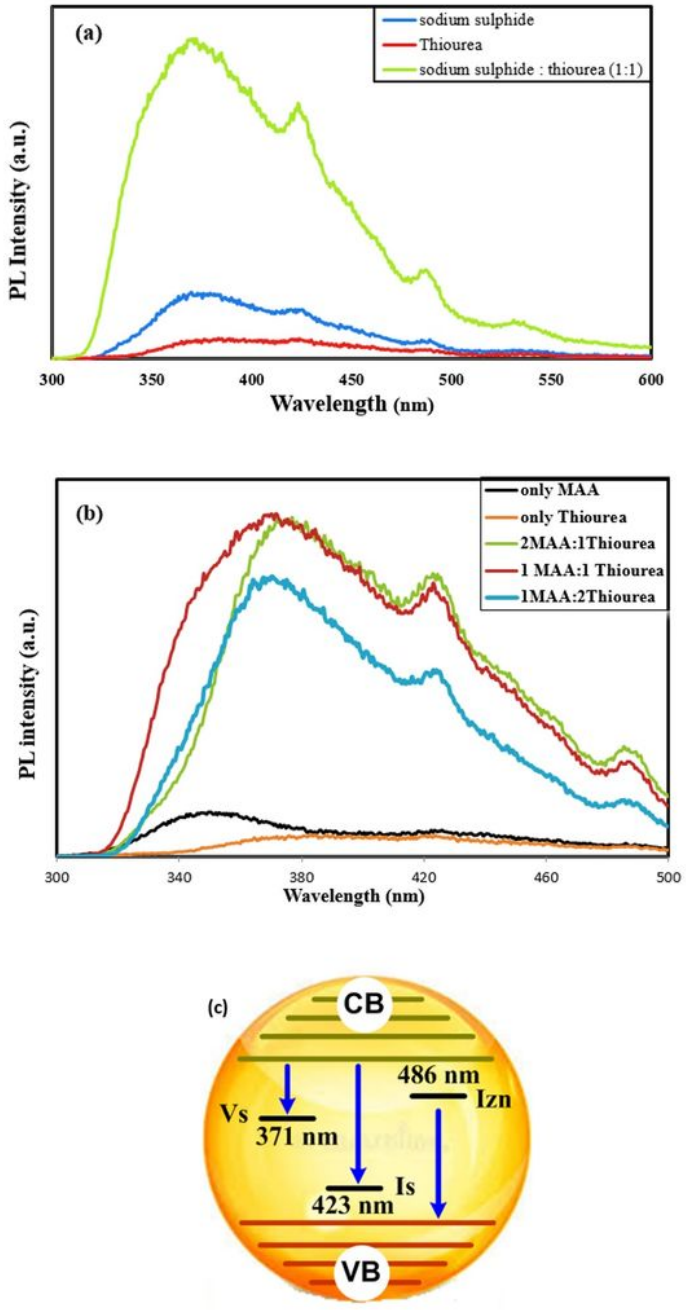

Figure 6

PL emission spectra of MAA capped-ZnS QDs prepared at different (a) source of sulfur, (b) molar ratios of MAA:thiourea, (c) Schematic energy level diagram of point defects in MAA capped-ZnS QDs. where: IS = interstitial sulfur, IZn= interstitial zinc and VZn= zinc vacancy,

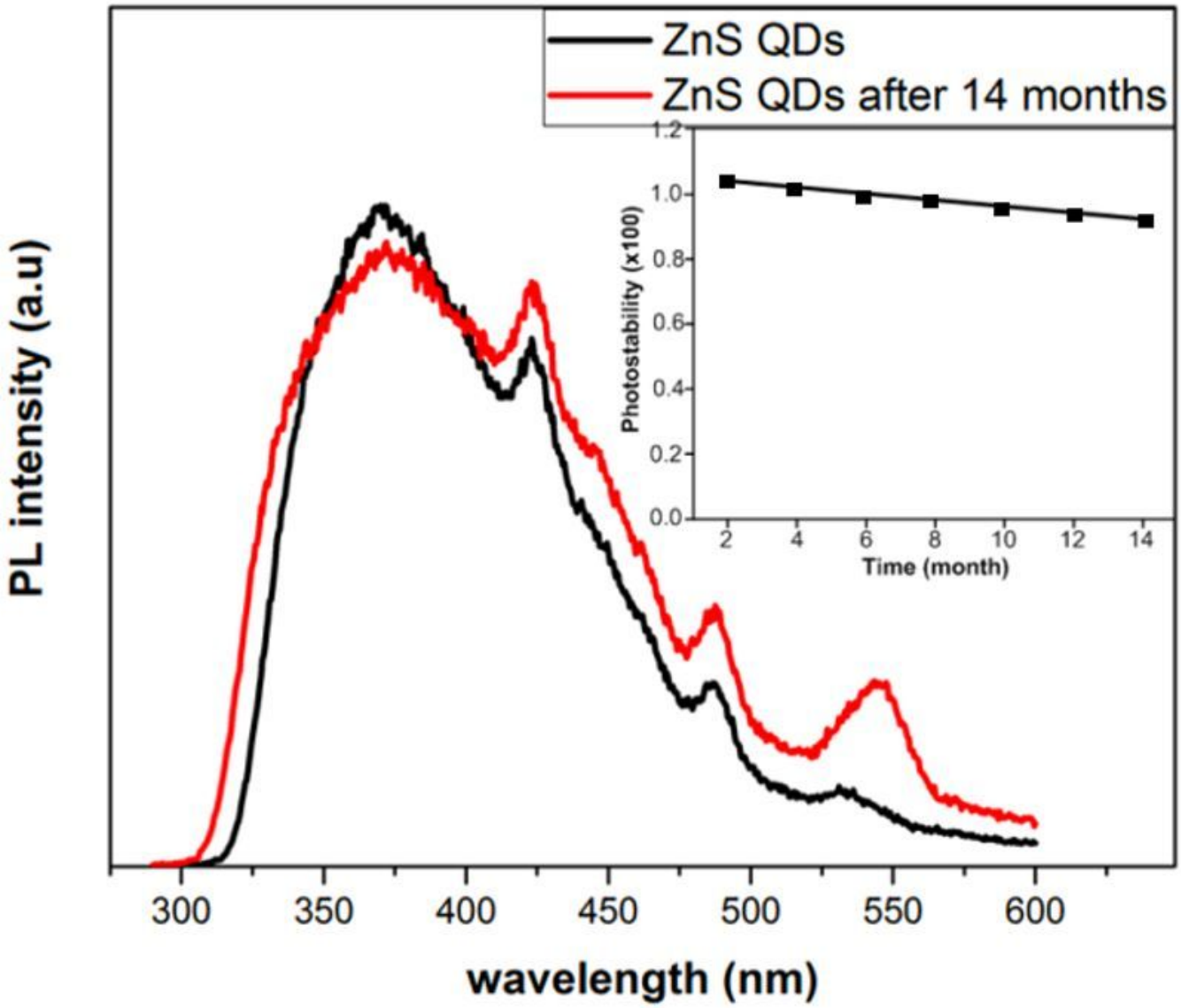

Figure 7

PL photostability of the MAA capped-ZnS QDs after 14 months, inset Photostability rate (×100) of MAA capped-ZnS QDs versus time.

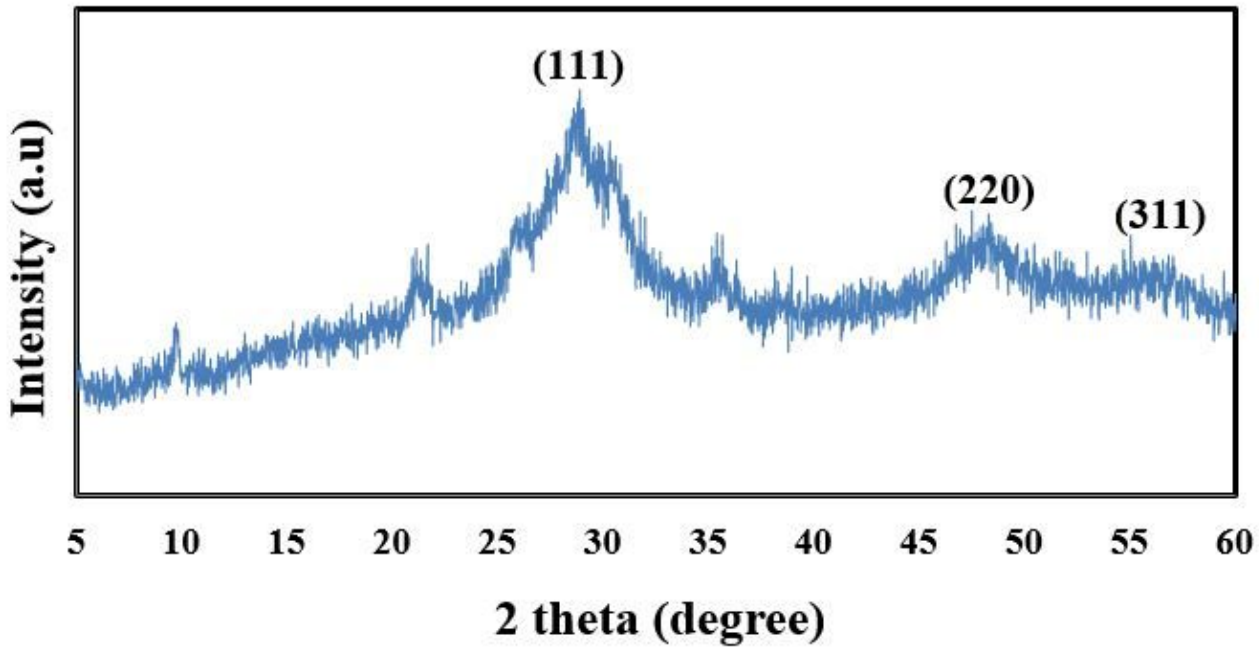

Figure 8

XRD pattern of MAA capped-ZnS QDs.

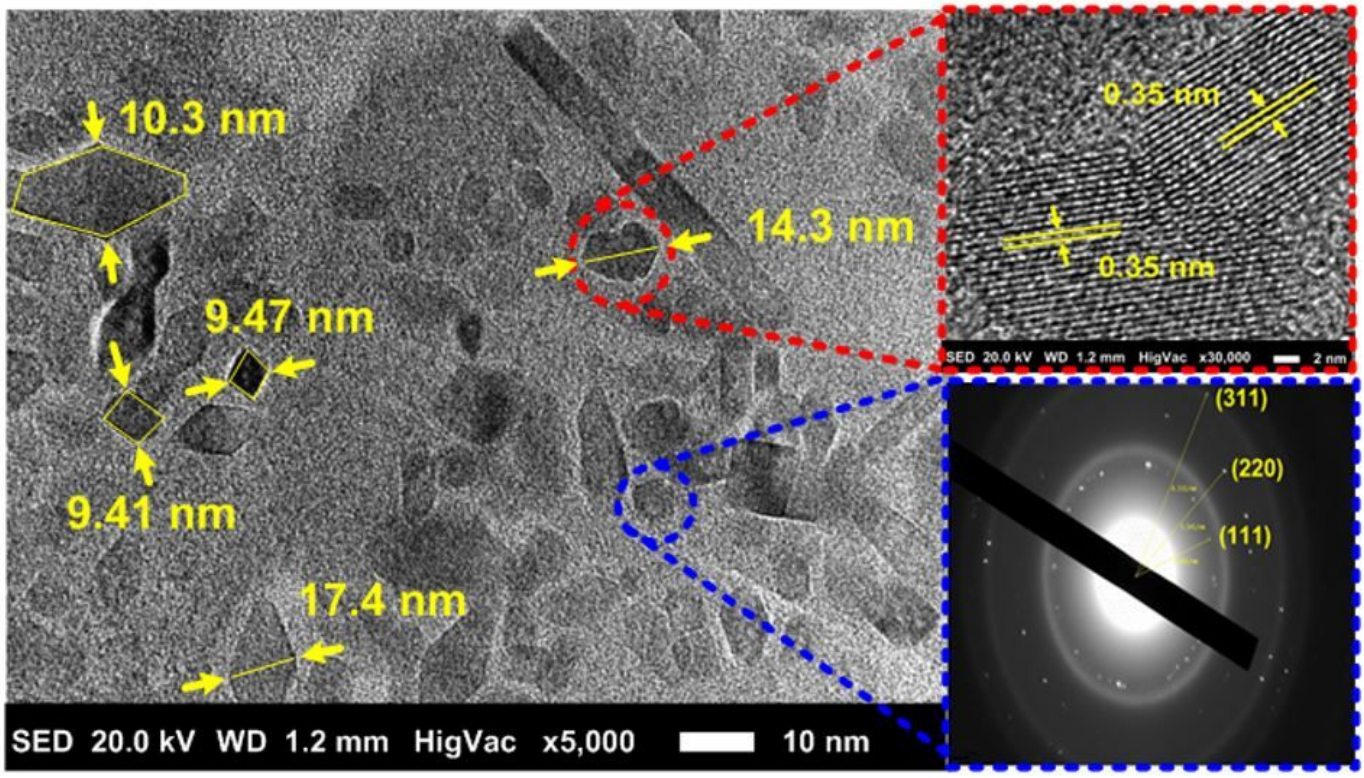

Figure 9

HRTEM images of MAA capped-ZnS QDs with high magnification image and SAED image were inserted as inset.

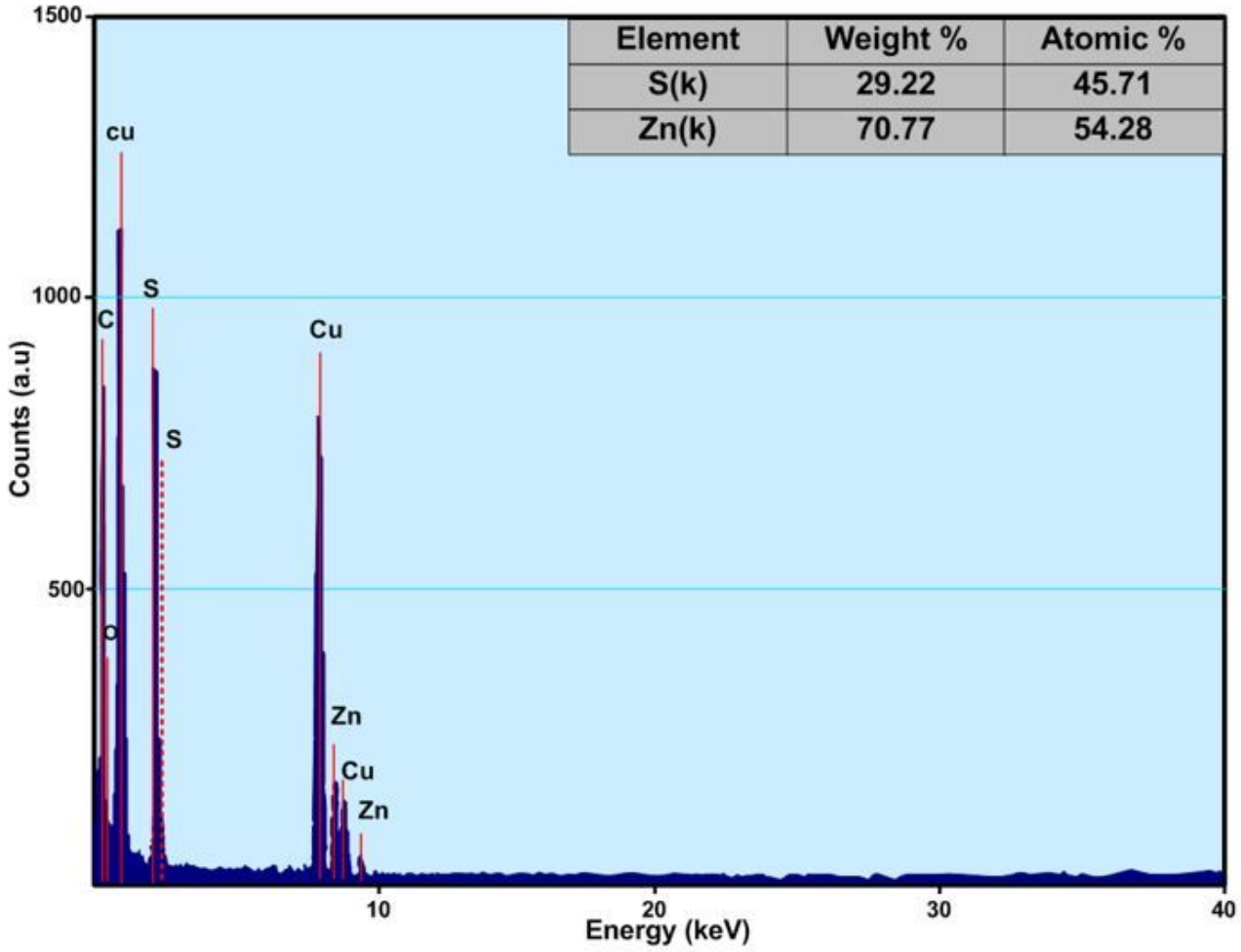

Figure 10

EDX of MAA capped-ZnS QDs. inset table declare the weight and atomic percentages of the Zn2+:S2- elements

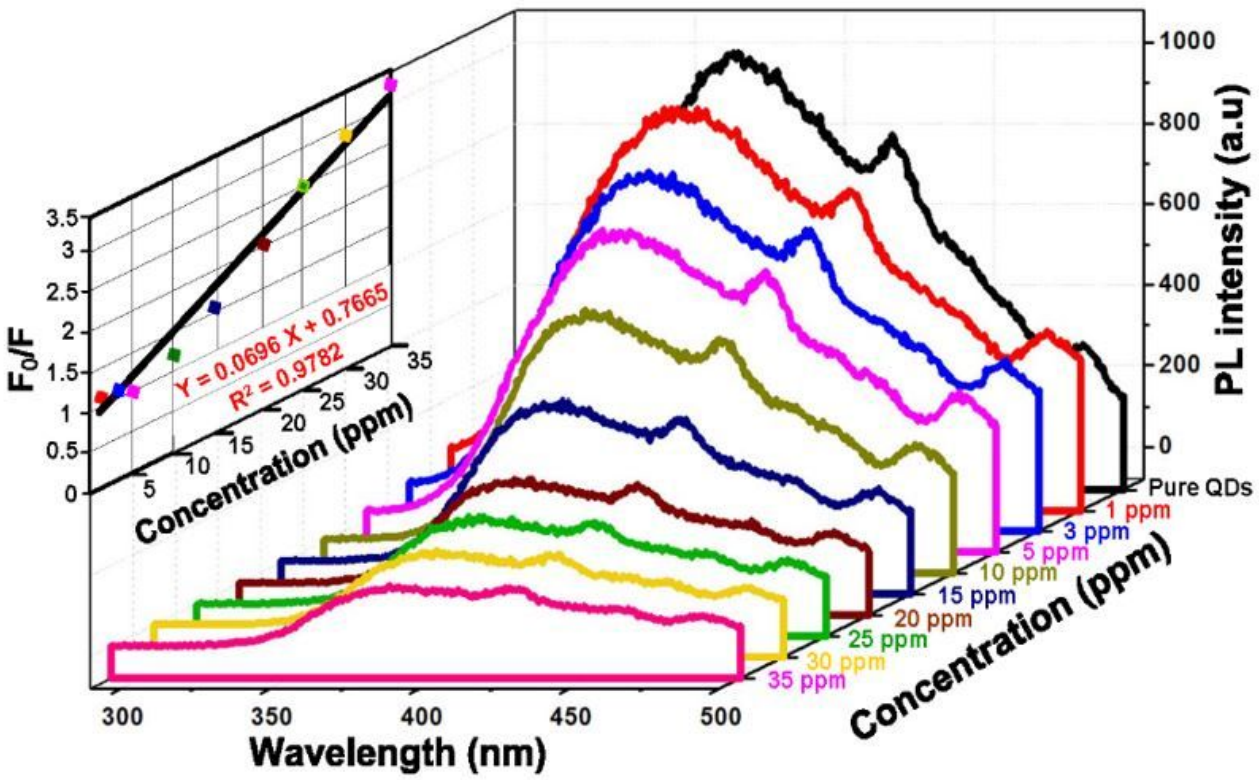

Figure 11

Stern-Volmer relationship between PL intensity of MAA capped-ZnS QDs and concentrations of free chlorine.

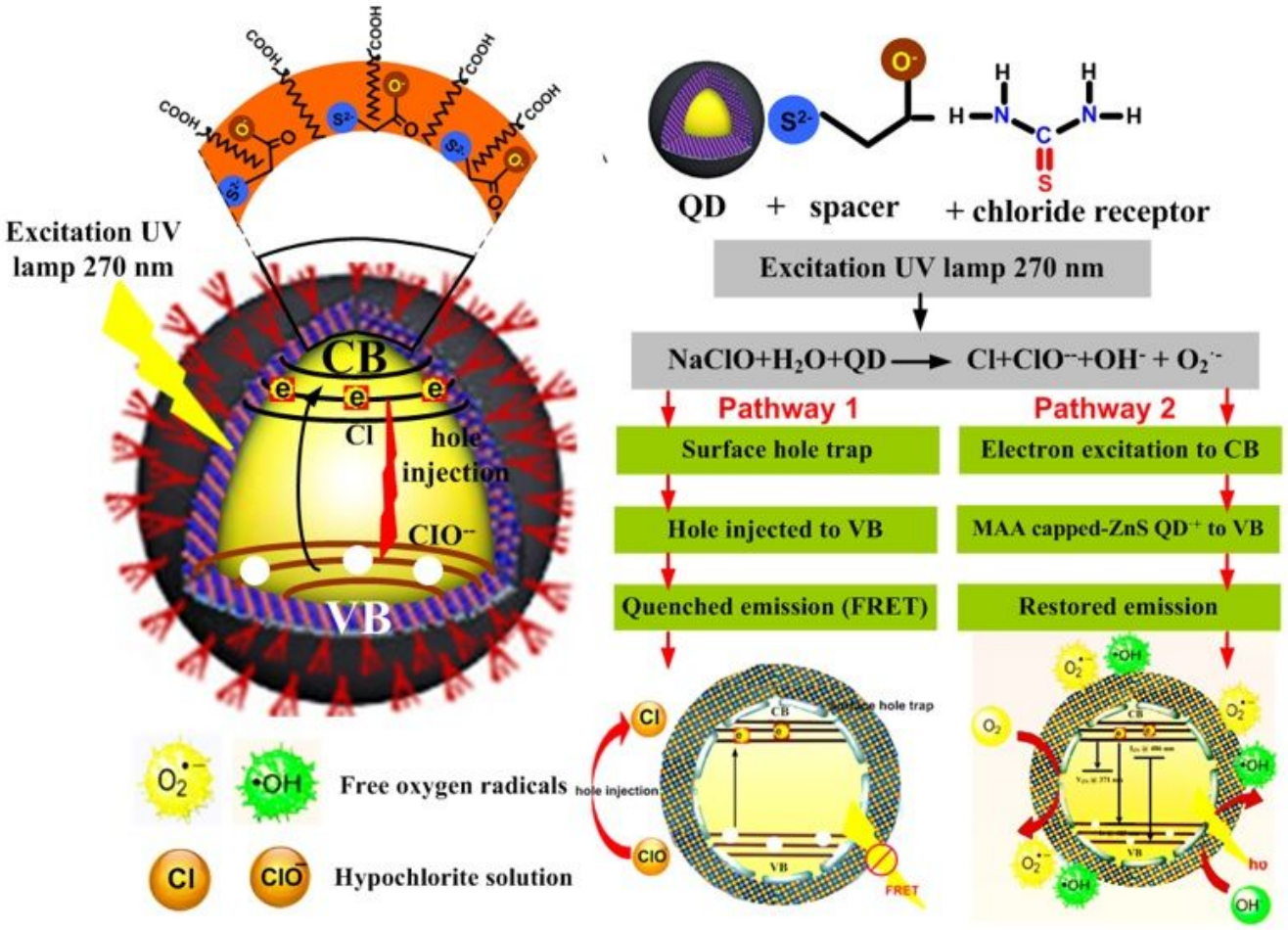

Figure 12

Schematic illustration of Cl2 mechanism of MAA capped-ZnS QDs/NaClO system